iScience

CellPress
OPEN ACCESS

Article

Metformin facilitates viral reservoir reactivation and their recognition by anti-HIV-1 envelope antibodies

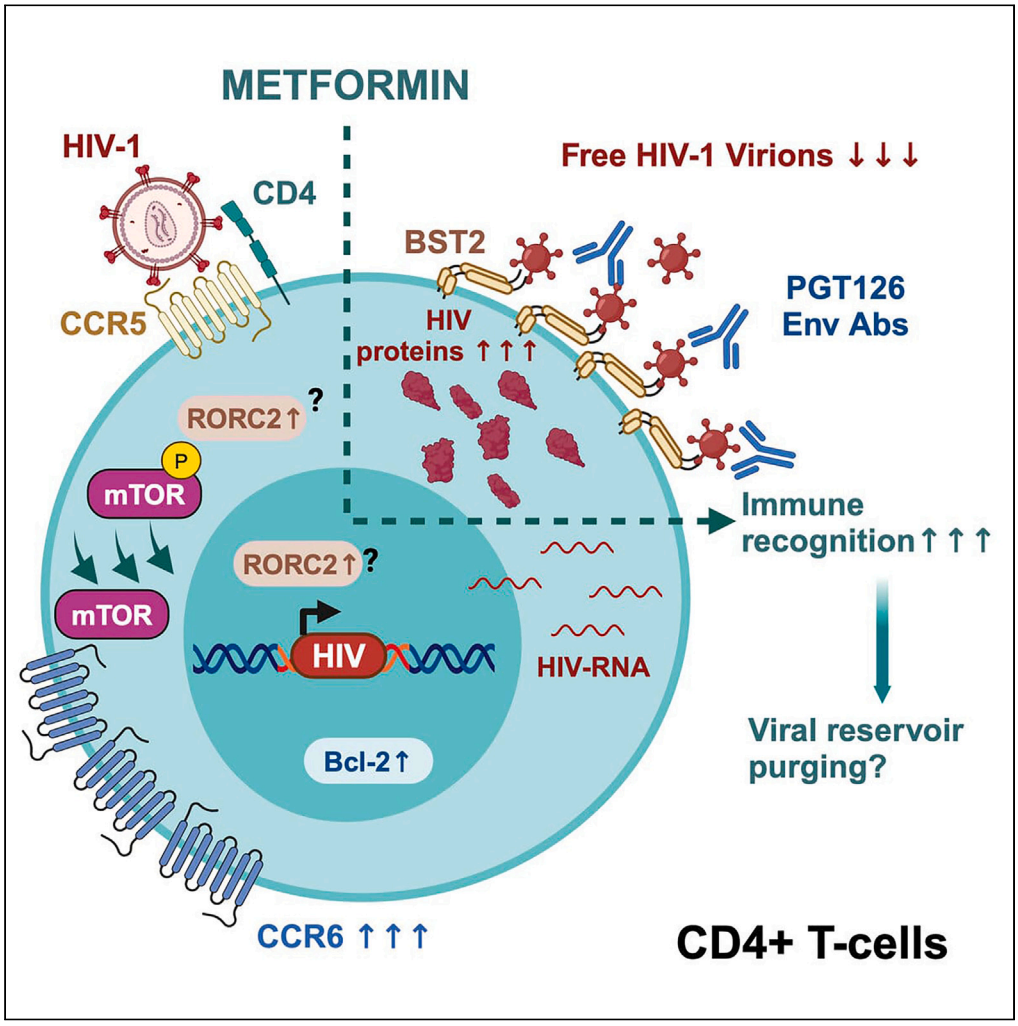

Augustine Fert, Jonathan Richard, Laurence Raymond Marchand, ..., Nicolas Chomont, Andrés Finzi, Petronela Ancuta

petronela.ancuta@umontreal.ca

Highlights

Metformin increases the frequency of productively HIV-infected T cells

Metformin acts on HIV-1 replication cycle at post-entry and post-integration levels

Metformin increases BST2 and Bcl-2 expression in productively HIV-infected T cells

Metformin increases viral reservoir recognition by anti-HIV-Env Abs

Fert et al., iScience *27*, 110670
September 20, 2024
https://doi.org/10.1016/j.isci.2024.110670

iScience

CellPress
OPEN ACCESS

Article

Metformin facilitates viral reservoir reactivation and their recognition by anti-HIV-1 envelope antibodies

Augustine Fert,[1,2] Jonathan Richard,[1,2] Laurence Raymond Marchand,[1] Delphine Planas,[1,2] Jean-Pierre Routy,[3,4,5] Nicolas Chomont,[1,2] Andrés Finzi,[1,2] and Petronela Ancuta[1,2,6,*]

SUMMARY

The mechanistic target of rapamycin (mTOR) positively regulates multiple steps of the HIV-1 replication cycle. We previously reported that a 12-week supplementation of antiretroviral therapy (ART) with metformin, an indirect mTOR inhibitor used in type-2 diabetes treatment, reduced mTOR activation and HIV transcription in colon-infiltrating CD4$^+$ T cells, together with systemic inflammation in nondiabetic people with HIV-1 (PWH). Herein, we investigated the antiviral mechanisms of metformin. In a viral outgrowth assay performed with CD4$^+$ T cells from ART-treated PWH, and upon infection *in vitro* with replication-competent and VSV-G-pseudotyped HIV-1, metformin decreased virion release, but increased the frequency of productively infected CD4^{low}HIV-p24$^+$ T cells. These observations coincided with increased BST2/tetherin (HIV release inhibitor) and Bcl-2 (pro-survival factor) expression, and improved recognition of productively infected T cells by HIV-1 envelope antibodies. Thus, metformin exerts pleiotropic effects on post-integration steps of the HIV-1 replication cycle and may be used to accelerate viral reservoir decay in ART-treated PWH.

INTRODUCTION

Antiretroviral therapy (ART) efficiently reduces HIV-1 replication to undetectable plasma levels and increases the life quality of people with HIV-1 (PWH).[1] However, ART does not eradicate HIV-1 since viral reservoirs (VRs) persist in cells and tissues, a process associated with increased risk of developing non-AIDS comorbidities such as cardiovascular diseases, cancers and metabolic disorders, thus causing accelerated aging (i.e., frailty, dementia).[2–6] Those HIV-1 related pathologies are caused by chronic immune activation.[7,8] Chronic immune activation in PWH is multifactorial. In fact, suboptimal ART penetration may occur in specific tissues and cell subsets.[9] In addition, ART does not restore mucosal CD4$^+$ T cells populations depleted by HIV-1 infection.[10] Finally, ART does not block HIV-1 transcription and translation leading to residual HIV-RNA and protein expression.[9,11,12] New therapeutic strategies are needed to reduce comorbidities associated with chronic inflammation in PWH. In the absence of an HIV cure, whether strategies targeting HIV transcription and translation could achieve this goal remains to be determined.

The mechanistic target of rapamycin (mTOR) pathway, a key regulator of T cell differentiation and growth via the induction of glycolysis,[13,14] was reported to be involved in multiple steps of the HIV-1 replication cycle (i.e., entry, reverse transcription, nuclear transport and transcription).[15–18] Previous work by our group demonstrated that mTOR expression and phosphorylation was preferentially induced in CD4$^+$ T cells expressing the Th17 marker CCR6 upon T cell receptor (TCR) triggering and exposure to the gut-homing modulator retinoic acid. Also, by using a VSV-G-pseudotyped HIV-1 construct, which enters cells via endocytosis independently of CD4 and co-receptors,[19] we demonstrated that mTOR activation facilitates the post-entry steps of the HIV-1 replication cycle in RA-treated CCR6$^+$CD4$^+$ T cells.[20] Furthermore, we demonstrated that mTOR inhibitors reduce viral outgrowth in CCR6$^+$CD4$^+$ T cells of ART-treated PWH.[20] Consistently, Besnard et al., showed that mTOR activation promotes HIV-1 transcription, via mechanisms involving the phosphorylating of CDK9, a subunit of the PTFEb complex, needed for HIV-1 transcription elongation.[17] Finally, Taylor et al. showed that mTOR activity is increased in CD4$^+$ T cells from ART-PWH compared to HIV-uninfected individuals; mTOR inhibition in TCR-activated CD4$^+$ T cells leads to a decrease in the pool of dNTPs needed for HIV-1 reverse transcription; and that mTOR activation stabilizes microtubules in HIV-infected T cells to facilitate the nuclear import of HIV-1 pre-integration complexes.[18]

[1]Centre de recherche du Centre hospitalier de l'Université de Montréal, Montréal, QC H2X 0A9, Canada
[2]Département de microbiologie, infectiologie et immunologie, Faculté de médecine, Université de Montréal, Montréal, QC H3C 3J7, Canada
[3]Infectious Diseases and Immunity in Global Health Program, Research Institute, McGill University Health Centre, Montréal, QC, Canada
[4]Chronic Viral Illness Service, McGill University Health Centre, Montréal, QC, Canada
[5]Division of Hematology, McGill University Health Centre, Montreal, QC, Canada
[6]Lead contact
*Correspondence: petronela.ancuta@umontreal.ca
https://doi.org/10.1016/j.isci.2024.110670

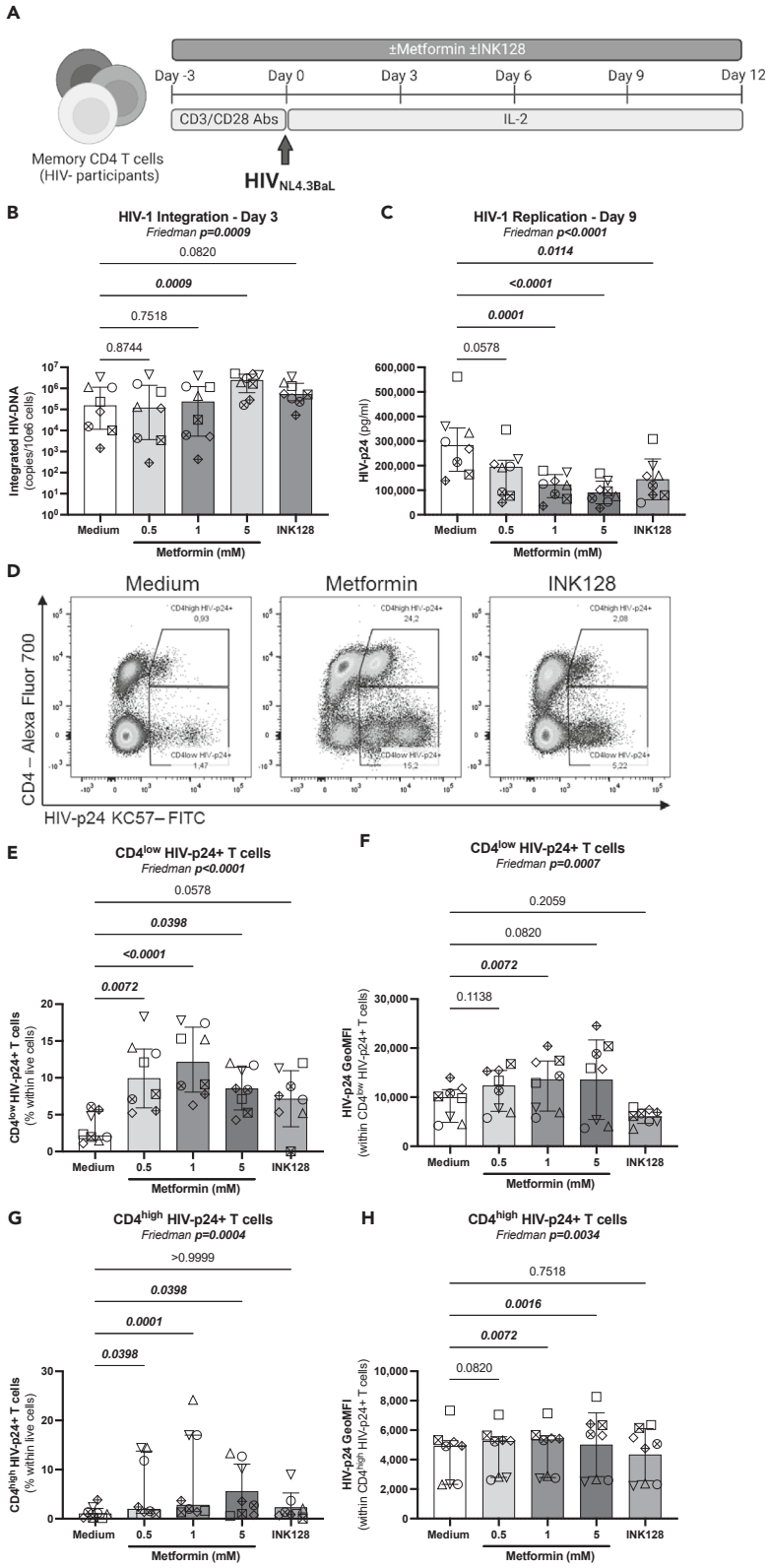
A
±Metformin ±INK128
Day -3
Day 0
Day 3
Day 6
Day 9
Day 12
CD3/CD28 Abs
IL-2
Memory CD4 T cells
(HIV- participants)
HIVNL4.3BaL
B
HIV-1 Integration - Day 3
Friedman p=0.0009
0.0820
0.0009
0.7518
0.8744
Integrated HIV-DNA
(copies/10e6 cells)
Medium
0.5
1
5
INK128
Metformin (mM)
C
HIV-1 Replication - Day 9
Friedman p<0.0001
0.0114
<0.0001
0.0001
0.0578
HIV-p24 (pg/ml)
D
Medium
Metformin
INK128
CD4 – Alexa Fluor 700
HIV-p24 KC57– FITC
E
CD4low HIV-p24+ T cells
Friedman p<0.0001
0.0578
0.0398
<0.0001
0.0072
CD4low HIV-p24+ T cells
(% within live cells)
F
CD4low HIV-p24+ T cells
Friedman p=0.0007
0.2059
0.0820
0.0072
0.1138
HIV-p24 GeoMFI
(within CD4low HIV-p24+ T cells)
G
CD4high HIV-p24+ T cells
Friedman p=0.0004
>0.9999
0.0398
0.0001
0.0398
CD4high HIV-p24+ T cells
(% within live cells)
H
CD4high HIV-p24+ T cells
Friedman p=0.0034
0.7518
0.0016
0.0072
0.0820
HIV-p24 GeoMFI
(within CD4high HIV-p24+ T cells)

Figure 1. Dose-response effects of metformin on HIV-1 replication in memory CD4$^+$ T cells *in vitro*

(A) Shown is the flow chart for the HIV-1 infection *in vitro*. Briefly, memory CD4$^+$ T cells from HIV-uninfected donors were stimulated with anti-CD3/CD28 Abs in the absence/presence of metformin (0.5, 1, or 5 mM) or INK128 (50 nM) for 3 days. Then, cells were exposed to the replication-competent NL4.3BaL HIV strain (50 ng HIV-p24/10^6 cells). Cell-culture supernatants were collected and media containing IL-2 and/or metformin or INK128 was refreshed every 3 days until day 12 post-infection. Shown are statistical analysis for integrated HIV-DNA levels were quantified by real-time nested PCR at day 3 post infection (B) and HIV-1 replication determined as HIV-p24 levels in cell-culture supernatants measured by ELISA at day 9 post-infection (C). Shown is a flow cytometry dot plot analysis of the intracellular HIV-p24 and surface CD4 expression allowing the identification of CD4^{low}HIV-p24$^+$ cells (productively infected) and CD4^{high}HIV-p24$^+$ cells in one representative donor (D); as well as the statistical analysis of CD4^{low}HIV-p24$^+$ T cell frequency (E) and their geometric MFI of HIV-p24 expression (F), and of CD4^{high}HIV-p24$^+$ T cell frequency (G) and their geometric MFI of HIV-p24 expression (H). Each symbol represents 1 donor (n = 8; median ± interquartile range). Friedman and uncorrected Dunn's multiple comparison p-values are indicated on the graphs.

Knowledge on the importance of mTOR pathway in regulating specific steps of the HIV-1 replication cycle,[15–18,20] prompted mTOR targeting *in vivo* in ART-treated PWH. In a single-arm clinical trial, 6-month supplementation of ART with everolimus, a direct mTOR inhibitor used as immunosuppressive drug in transplant recipient,[21] decreased mTOR activation, as well as the cell-associated (CA) HIV-RNA levels in blood CD4$^+$ T cells,[22] thus pointing to a potential direct role of mTOR in modulating HIV transcription *in vivo*. However, the use of such immunosuppressive drugs is not recommended outside organ transplantation. Metformin, an indirect mTOR inhibitor, is a drug approved by the Food and Drug Administration (FDA) and widely used to treat type-2 diabetes.[23] Mechanistically, metformin blocks the first complex of the respiratory chain of the mitochondria, leading to an increase in the AMP/ATP ratio. The change in this ratio leads to an activation of AMP-activated protein kinase pathway, which results in mTOR pathway inhibition.[24,25] Our group performed a pilot non-randomized clinical trial in which non-diabetic ART-treated PWH received metformin for 12 weeks, and matched blood and colon biopsies were collected at baseline and the end of treatment for immunological and virological measurements.[26,27] Metformin significantly decreased the frequency of colon-infiltrating CD4$^+$ T cells and mTOR phosphorylation in CCR6$^+$CD4$^+$ T cells, and reduced levels of systemic inflammation (i.e., sCD14). Finally, a reduction in HIV-1 transcription, measured as the HIV-RNA/DNA ratio, was observed in CD4$^+$ T cells isolated from the colon in a fraction of study participants (8/13), thus pointing to a potential link between mTOR activation and HIV-1 transcription in T cells carrying VRs.[27] Of interest, Guo et al. showed that metformin reduced HIV-1 replication and limited CD4$^+$ T cells depletion in a humanized mouse model reconstituted with primary human CD4$^+$ T cells.[28] Another study showed that 24 weeks of metformin administration in complement of ART decreased the frequency of CD4$^+$ T cells with a PD1$^+$TIGIT$^+$TIM3$^+$ phenotype considered as a molecular signature for exhausted cells contributing to HIV persistence.[29,30] Whether the metformin supplementation of ART may represent a valuable strategy to decrease immune dysfunction in PWH requires further investigations.

Given the encouraging results of metformin supplementation of ART in PWH,[27,31] we sought to identify the steps of the HIV-1 replication cycle modulated by metformin and its mechanisms of action. To this aim, we studied the effects of metformin on HIV-1 replication in CD4$^+$ T cells from HIV-uninfected participants exposed to HIV-1 *in vitro*. Also, we tested metformin effects on viral outgrowth from CD4$^+$ Tcells of ART-treated PWH. Our results reveal unexpected effects of metformin on various post-entry steps of the viral replication cycle. Metformin increased HIV-p24 expression at single-cell level upon HIV-infection *in vitro*, without a proportional increase in HIV-DNA integration and viral release, via mechanisms involving increased BST2/tetherin (HIV release inhibitor) and Bcl-2 (pro-survival factor) expression. Also, metformin favored the recognition of reactivated HIV-1 reservoir cells by broadly neutralizing (bNAbs) anti-HIV-Env Abs. Overall, these results support a model in which metformin may be used to accelerate VR decay during ART.

RESULTS

Metformin dose-response testing

To determine the optimal concentration of metformin for experiments *in vitro*, we first tested the effect of different doses of metformin on the phosphorylation of mTOR and its downstream substrate, the ribosomal S6 (S6). Results demonstrate that metformin at 1 mM efficiently inhibited mTOR and S6 phosphorylation upon TCR triggering, without impacting on cell viability and proliferation, while metformin at 5 mM reduced proliferation and viability (Figure S1). Thus, the dose of 1 mM metformin was considered optimal for CD4$^+$ T cells *in vitro*. A similar concentration of metformin (1 mM) showed efficacy in another study in blocking the mTOR pathway and HIV-1 replication by reducing oxygen consumption in CD4$^+$ T cells.[28]

Metformin increases the frequency of HIV-p24$^+$ T cells without a proportional increase in viral release upon infection *in vitro*

To explore metformin effects on HIV-1 replication, TCR-stimulated CD4$^+$ T cells from HIV-uninfected participants were exposed to a replication-competent CCR5-tropic HIV$_{NL4.3BAL}$ virus upon TCR triggering and culture, in the presence or the absence of metformin (0.5, 1, 5 mM) and INK128 (50 nM), a potent direct mTORC1/mTORC2 inhibitor[32] (Figure 1A). Although metformin (1 mM) and INK128 treatment did not significantly impact on levels of HIV-DNA integration at day 3 post-infection (Figure 1B), both reduced HIV-p24 levels in cell-culture supernatant, with metformin showing a dose-response effect (Figure 1C). Cells treated with 5 mM of metformin displayed higher integrated HIV-DNA levels (Figure 1B), however, this concentration reduced cell viability and proliferation (Figures S1E and S1F). Flow cytometry analysis at day 12 post-infection reveals that metformin increased intracellular HIV-p24 expression in T cells with a CD4^{low} phenotype (productively infected) or CD4^{high} (likely bystander cells coated with newly formed virions) (Figure 1D). The HIV accessory proteins Nef and Vpu downregulate CD4,[33,34] and their presence in HIV$_{NL4.3BAL}$ explains the downregulation of CD4 on the surface of productively infected T cells.

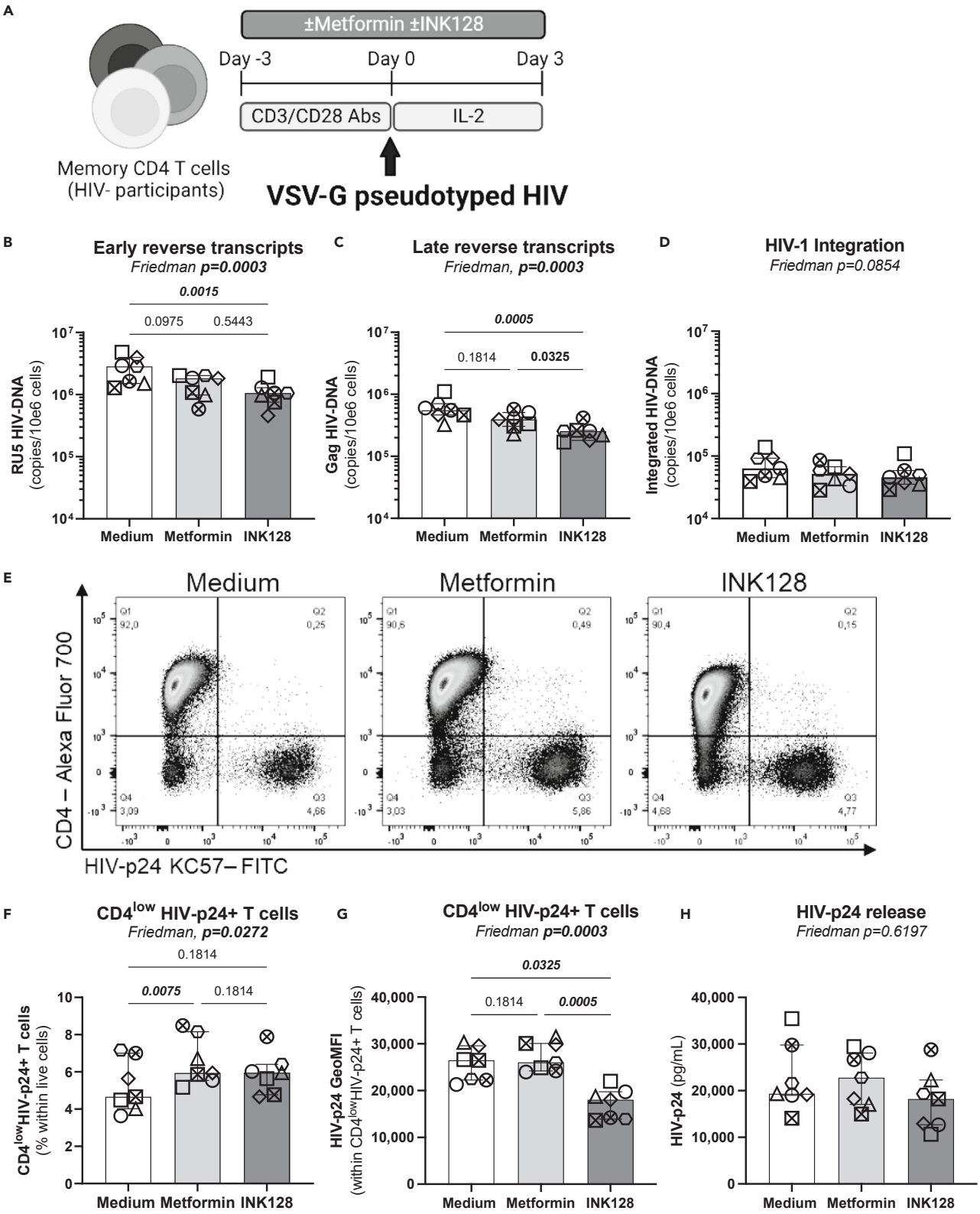
A
±Metformin ±INK128
Day -3
Day 0
Day 3
CD3/CD28 Abs
IL-2
Memory CD4 T cells
(HIV- participants)
VSV-G pseudotyped HIV
B
Early reverse transcripts
Friedman p=0.0003
0.0015
0.0975
0.5443
RU5 HIV-DNA
(copies/10e6 cells)
Medium
Metformin
INK128
C
Late reverse transcripts
Friedman, p=0.0003
0.0005
0.1814
0.0325
Gag HIV-DNA
(copies/10e6 cells)
D
HIV-1 Integration
Friedman p=0.0854
Integrated HIV-DNA
(copies/10e6 cells)
E
Medium
Metformin
INK128
CD4 – Alexa Fluor 700
HIV-p24 KC57– FITC
F
CD4low HIV-p24+ T cells
Friedman, p=0.0272
0.1814
0.0075
CD4lowHIV-p24+ T cells
(% within live cells)
G
CD4low HIV-p24+ T cells
Friedman p=0.0003
0.0325
HIV-p24 GeoMFI
(within CD4lowHIV-p24+ T cells)
H
HIV-p24 release
Friedman p=0.6197
HIV-p24 (pg/mL)

Figure 2. Effects on metformin on single-round HIV-1 infection *in vitro*

(A) Shown is the flow chart for the single-round HIV-1 infection *in vitro*. Briefly, memory CD4$^+$ T cells from HIV-uninfected donors were stimulated by anti-CD3/CD28 Abs in the absence/presence of metformin (1 mM) or INK128 (50 nM) for 3 days. Then, cells were exposed to a replication-incompetent single-round VSV-G-pseudotyped HIV-1 construct (100 ng HIV-p24/10^6 cells). Cell-culture supernatants and cells were collected at day 3 post-infection. Shown are levels of early (RU5) (B) and late HIV reverse transcripts (Gag) (C), as well as integrated HIV-DNA (D) quantified by real-time nested PCR. Shown are representative flow cytometry dot plots of intracellular HIV-p24 and surface CD4 expression from one donor (E) and statistical analysis of the productively infected CD4^{low}HIV-p24$^+$ T cells in terms of frequencies (F) and the geometric MFI of HIV-p24 expression (G). Shown are absolute HIV-p24 levels in cell culture supernatants quantified by ELISA (H). Each symbol represents one donor ($n = 7$; median ± interquartile range). Friedman and uncorrected Dunn's multiple comparison p values are indicated on the graphs.

Also, CD4 downregulation precedes HIV-p24 expression,[33,34] likely explaining the detection of a CD4^{low}HIV-p24$^-$ population (Figure 1D). It is also noteworthy the atypical appearance of two subsets of CD4^{low}HIV-p24$^+$ T cells, with medium and high levels of HIV-p24 expression upon exposure to metformin (Figure 1D). In contrast to results in Figure 1C, metformin, at 1 mM dose, increased cell-associated HIV-p24 levels in terms of frequency of CD4^{low}HIV-p24$^+$ and intensity of HIV-p24 expression (Figures 1E and 1F). Metformin also significantly increased the frequency of CD4^{high}HIV-p24$^+$ T cells, as well as the intensity of HIV-p24 expression (Figures 1G and 1H).

In conclusion, these results demonstrate that metformin increases cell-associated HIV-p24 expression and results in the expansion of HIV-p24$^+$ T cells with CD4^{low} and CD4^{high} phenotypes, likely by promoting HIV-1 cell-to-cell transmission via mechanisms independent of free-virion release.

Effects of metformin on RORC2 expression and IL-17A production

Studies by our group and others demonstrating that Th17 cells are highly permissive to HIV-1 infection[35–37] prompted us to investigate the effect of metformin on Th17 polarization. Results show that metformin acted on memory CD4$^+$ T cells from uninfected participants to increase the frequency and intensity of RORC2 and CCR6 expression at single-cell level, enhanced the frequency of RORC2$^+$CCR6$^+$ T cells (Figures S2A–S2F), and maintained T cell capacity to produce IL-17A in response to TCR triggering upon culture *in vitro* (Figures S2G and S2H). In contrast, INK128 did not increase RORC2 expression and the frequency of RORC2$^+$CCR6$^+$ T cells (Figures S2A–S2F), and decreased IL-17A production early upon TCR triggering (Figures S2G and S2H). Thus, the effects of metformin on cell-associated HIV-p24 expression coincide with the promotion of a Th17 phenotype and the preservation of Th17 effector functions in memory CD4$^+$ T cells.

Effects of metformin on CD4, CCR5, and CXCR4 expression

To get insights into the molecular mechanisms underlying differences between metformin and INK128, cells were analyzed for the expression of the HIV-1 entry receptor CD4, and co-receptors CCR5 and CXCR4. Metformin did not impact on CD4 and CXCR4 surface protein expression, while INK128 slightly decreased CD4 and increased CXCR4, mainly in terms of geometric MFI at single-cell level (Figures S3A and S3B). Levels of CCR5 mRNA expression tended to decrease, with differences reaching statistical significance in matched comparisons for INK128, but not metformin versus medium (Figure S3C). Thus, the effects of metformin on HIV-1 replication appear independent of the modulation of viral entry receptors and co-receptors.

Metformin facilitates HIV-1 replication post-integration and prior to viral release

To localize the step(s) of the HIV-1 replication cycle affected by metformin, single-round infection with a VSVG-pseudotyped HIV-1 (HIV$_{VSV-G}$), with GFP in place of Env, but encoding for functional Nef and Vpu, was performed on memory CD4$^+$ T cells from HIV-uninfected participants in the presence/absence of metformin (1 mM) or INK128 (50 nM) (Figure 2A). In agreement with results in Figure 1, metformin did not significantly modify levels of early and late reverse transcripts, nor HIV-DNA integration (Figures 2B–2D), supporting the idea that metformin acts at post-integration level(s). In contrast, INK128 significantly reduced levels of RU5 and Gag HIV-DNA (Figures 2B and 2C) metformin slightly increased the frequency of CD4^{low}HIV-p24$^+$ T cells without significantly enhancing the intensity of HIV-p24 expression *per* cell (Figures 2E–2G). In this model of single-round infection, where cell-to-cell transmission does not occur given the absence of Env on the surface of progeny virions, the CD4^{high}HIV-p24$^+$ T cell population was not observed (Figure 2E), likely since Env-deficient virions cannot bind to new cells. Similar to results in Figure 1, metformin did not proportionally increase the HIV-p24 release in cell-culture supernatants (Figure 2H). In contrast, INK128 diminished the intensity of HIV-p24 expression at single-cell level, although it exerted no effect on HIV-p24 levels in cell-culture supernatants (Figures 2F–2H). These results suggest that metformin acts at post-integration levels by facilitating cell-associated HIV-p24 expression, with no effect on viral release.

Metformin promotes VR reactivation in memory CD4$^+$ T cells of ART-treated PWH

To explore the effect of metformin (1 mM) on the reactivation of HIV-1 reservoirs that persist during ART in PWH, we performed a simplified viral outgrowth assay (VOA),[38] as depicted in Figure 3A, using cells from ART-treated PWH ($n = 11$; Table 1) (Figure 3). In the absence of ARVs, the mTOR inhibitor INK128 significantly reduced viral outgrowth, as reflected by levels of integrated HIV-DNA in cells and HIV-p24 levels in cell-culture supernatants, as well as intracellular HIV-p24 expression (Figures 3B–3E, left panels), consistent with the antiviral effects of INK128 previously reported by our group and others.[15,20] Unexpectedly, under these same experimental conditions, metformin did not decrease HIV-DNA integration at day 12 in culture, nor viral release in cell-culture supernatants (Figures 3B and 3C, left panels). In contrast, a tendency for a metformin-mediated increase in HIV-DNA integration was observed, with median levels changing from 4,478 to 11,830 integrated HIV-DNA

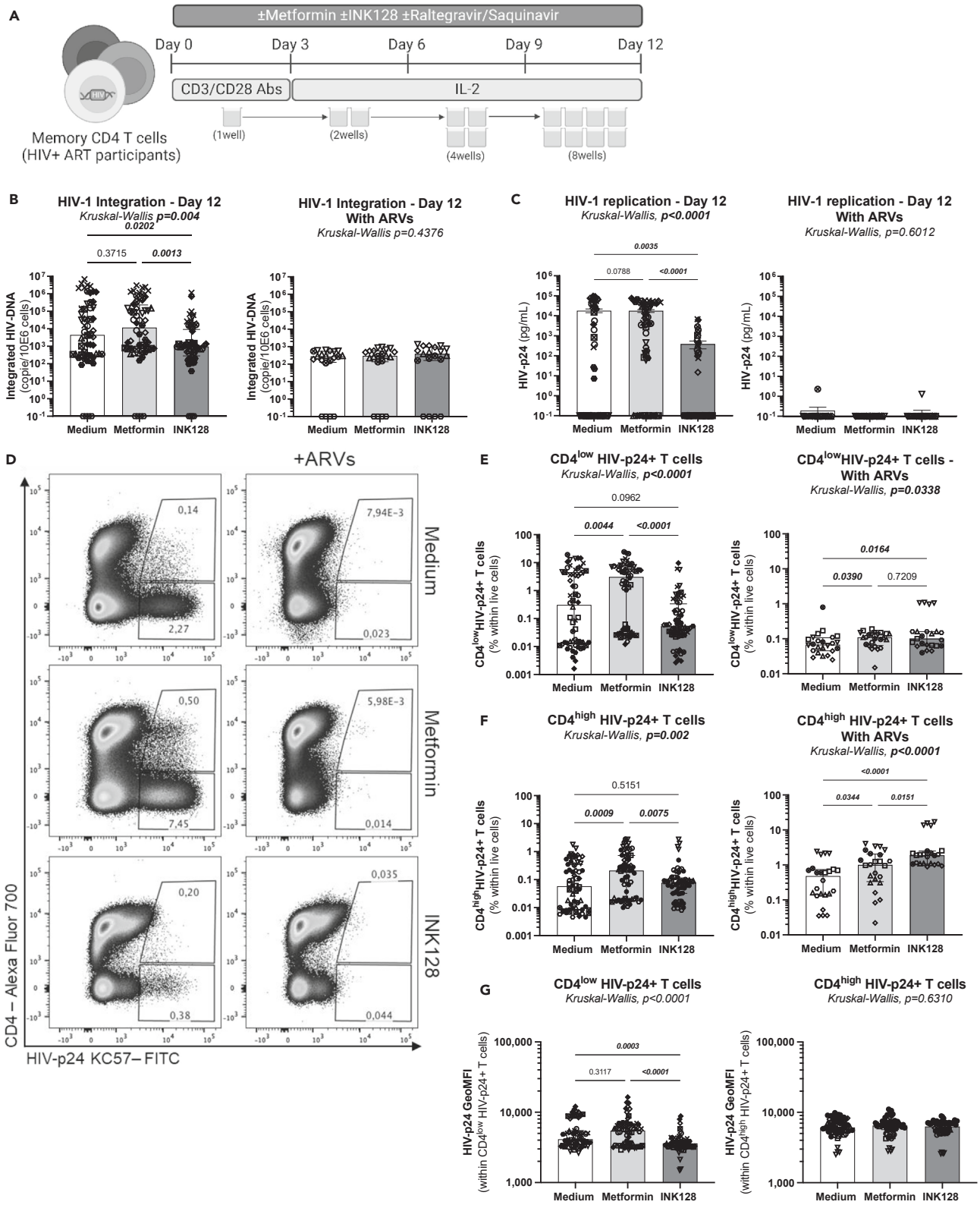
A
±Metformin ±INK128 ±Raltegravir/Saquinavir
Day 0
Day 3
Day 6
Day 9
Day 12
CD3/CD28 Abs
IL-2
Memory CD4 T cells
(HIV+ ART participants)
(1well)
(2wells)
(4wells)
(8wells)
B
HIV-1 Integration - Day 12
Kruskal-Wallis p=0.004
0.0202
0.3715
0.0013
Integrated HIV-DNA (copie/10E6 cells)
Medium
Metformin
INK128
HIV-1 Integration - Day 12
With ARVs
Kruskal-Wallis p=0.4376
C
HIV-1 replication - Day 12
Kruskal-Wallis, p<0.0001
0.0035
0.0788
<0.0001
HIV-p24 (pg/mL)
HIV-1 replication - Day 12
With ARVs
Kruskal-Wallis, p=0.6012
D
+ARVs
Medium
Metformin
INK128
0,14
2,27
7,94E-3
0,023
0,50
7,45
5,98E-3
0,014
0,20
0,38
0,035
0,044
CD4 – Alexa Fluor 700
HIV-p24 KC57– FITC
E
CD4low HIV-p24+ T cells
Kruskal-Wallis, p<0.0001
0.0962
0.0044
<0.0001
CD4lowHIV-p24+ T cells (% within live cells)
CD4lowHIV-p24+ T cells - With ARVs
Kruskal-Wallis, p=0.0338
0.0164
0.0390
0.7209
F
CD4high HIV-p24+ T cells
Kruskal-Wallis, p=0.002
0.5151
0.0009
0.0075
CD4highHIV-p24+ T cells (% within live cells)
CD4high HIV-p24+ T cells With ARVs
Kruskal-Wallis, p<0.0001
<0.0001
0.0344
0.0151
G
CD4low HIV-p24+ T cells
Kruskal-Wallis, p<0.0001
0.0003
0.3117
<0.0001
HIV-p24 GeoMFI (within CD4low HIV-p24+ T cells)
CD4high HIV-p24+ T cells
Kruskal-Wallis, p=0.6310
HIV-p24 GeoMFI (within CD4high HIV-p24+ T cells)

Figure 3. Effects of metformin on viral outgrowth in memory CD4$^+$ T cells from ART-treated PWH

(A) Shown is the flow chart for the viral outgrowth assay (VOA). Briefly, memory CD4$^+$ T cells from ART-treated PWH were stimulated with CD3/CD28 Abs, in the presence (n = 11) or the absence (n = 6) of ARVs and in the presence/absence of metformin (1 mM) or INK128 (50 nM) for 3 days. Supernatants were collected, cells were split in two news wells, and media containing IL-2 and metformin or INK128 was refreshed every 3 days. Experiments were performed in 4–8 original replicates *per* condition. One original replicate at day 0 generated 8 final replicates at day 12. At the end of the experiment, T cells derived from the same original replicate were merged for PCR and flow cytometry analysis. Shown are (B) integrated HIV-DNA levels quantified by real-time nested PCR and (C) levels of HIV-p24 in cell-culture supernatants quantified by ELISA. Shown are (D) representative flow cytometry dot plot of cell-associatedHIV-p24 and surface CD4 expression; (E) statistical analysis of the frequency of CD4^{low}HIV-p24$^+$, (F) the frequency of CD4^{high}HIV-p24$^+$ cells; and (G) the geometric MFI (GeoMFI) of HIV-p24 expression in CD4^{low} HIV-p24$^+$ and CD4^{high} HIV-p24$^+$ T cell subsets. Each symbol represents one donor; bars indicate the median ± interquartile range. Kruskal-Wallis test and uncorrected Dunn's multiple comparison p values are indicated on the graphs.

copies/10^6 T cells in the absence and the presence of metformin, respectively (Figure 3B, left panels). Similarly, HIV-p24 levels in cell culture supernatants were slightly increased by metformin (p = 0.0788) (Figure 3C, left panels). Metformin robustly increased the frequency of productively infected cells, identified as cells with a CD4^{low}HIV-p24$^+$ phenotype (Figures 3D and 3E, left panels). Metformin also increased the frequency of a relatively small subset of CD4^{high}HIV-p24$^+$ T cells (Figures 3D and 3F, left panels). There was no increase in the geometric MFI of HIV-p24 expression within CD4^{low}HIV-p24$^+$ and CD4^{high}HIV-p24$^+$ T cells (Figure 3G, left panel). These results demonstrate that metformin facilitates the expansion of productively infected cells upon TCR-triggering *in vitro*, without a proportional increase in the release of free progeny virions in cell-culture supernatants as observe in the context of HIV infection *in vitro*.

For a fraction of 6 out of 11 ART-treated PWH, experiments were performed in parallel in the presence of ARVs (integrase inhibitor Raltegravir; protease inhibitor Saquinavir), to block the infection of new cells by progeny virions produced upon TCR-mediated VR reactivation (Figure 3). Results in Figure 3B reveal, a strong decrease in integrated HIV-DNA levels mediated by ARVs in all three conditions, with the abrogation of differences between medium and metformin versus INK128 observed in the absence of ARVs. Similarly, in the presence of ARVs, soluble and cell-associated HIV-p24 levels were dramatically decreased in all three conditions (Figures 3C–3E). Thus, the proviral effects of metformin were abrogated in the presence of ARVs, which block cell-to-cell transmission of virions newly produced by reactivated VR *in vitro*. Together these results support a model in which metformin exerts its proviral effects by facilitating cell-to-cell transmission independently of cell-free virion release, consistent with previous reports.[39,40]

To get more mechanistic insights into the metformin mechanism of action in the VOA performed in the absence of ARVs, cells harvested at day 12 post-TCR triggering were analyzed for the expression of RORC2, CCR6, and IL-17A. Metformin versus medium increased the frequency of RORC2$^+$ and CCR6$^+$ T cells and the intensity of RORC2 and CCR6 expression at single-cell level (Figures S4A–S4C). Also, metformin versus medium slightly increased the frequency of CD4$^+$ T cells co-expressing RORC2 and CCR6, identified as Th17-like cells (Figures S4A and S4D), but had no effect IL-17A production in cell-culture supernatants (Figure S4E). For INK128 versus medium, despite an increase in the frequency of cells expressing CCR6 (Figures S4A and S4C), and a tendency for an increase in the frequency of RORC2-expressing cells (p = 0.0856) (Figures S4A and S4B), there was a significant reduction in IL-17A production in cell-culture supernatants (Figure S4E). Thus, metformin increased the frequency of CD4$^+$ T cells with a Th17 phenotype (Figure S4D), without proportionally increasing their effector functions (i.e., IL-17A production).

These results reveal that, in contrast to INK128 that inhibits both HIV-1 outgrowth and IL-17A production, metformin increases the frequency of T cells expressing cell-associated HIV-p24 via mechanisms independent on free-virion release and maintains Th17 functions. These observations raise new questions on the effects of metformin on specific post-integration steps of the HIV-1 replication cycle.

Metformin increases surface expression of BST2 on productively infected T cells *in vitro*

HIV-1 release is controlled by complex mechanisms, including BST2, a protein that sequester newly formed viral particles at the cell-surface membrane.[41,42] The HIV-1 accessory protein Vpu counteracts the effects of BST2 by inducing its downregulation[42,43] or displacement from the site of viral assembly,[44] with BST2 mediating cell-to-cell transmission of Vpu-defective HIV-1 virions.[39] Considering the discrepancy between the effects of metformin on the frequency of productively infected cells and virion release, we hypothesized that metformin limits virion release and facilitate their cell-to-cell transmission by promoting BST2 expression. To test the possibility, memory CD4$^+$ T cells harvested at day 12 post-infection with HIV-1 $_{NL4.3Bal}$ *in vitro* (Figure 1A) and memory CD4$^+$ T cells of ART-treated PWH harvested at day 12 post-TCR triggering (Figure 3A) were analyzed for surface expression of BST2 and cell-associated HIV-p24. Results in representative donors depicted in Figure 4A reveal the typical down regulation of BST2 on productively infected T cells. Further, the expression of BST2 was analyzed on productively infected (CD4^{low}HIV-p24$^+$) versus uninfected (CD4$^+$HIV-p24$^-$) T cells upon HIV$_{NL4.3BaL}$ infection *in vitro* (Figures 4B and 4C), in VOA (Figures 4D and 4E), and in uninfected CD4$^+$ T cells (Figure 4F). Upon HIV$_{NL4.3BaL}$ infection *in vitro*, metformin and INK128 significantly increased BST2 expression at the surface of productively infected, but not uninfected T cells (Figures 4B and 4C). In contrast, INK128 but not metformin increased surface BST2 expression on productively infected T cells in VOA (Figures 4D and 4E). The upregulation of BST2 was not observed when uninfected memory CD4$^+$ T cells were exposed to metformin or INK128 (Figure 4F).

These results reveal that metformin prevents the HIV-mediated downregulation of surface BST2 expression on productively infected cells, only upon exposure to HIV-1 *in vitro*, while INK128 demonstrated to be a robust modulator of surface BST2 expression in VOA as well. The fact that metformin and INK128 failed to modulate BST2 expression in the absence of HIV-1 exposure points to an HIV-dependent mechanisms of action for metformin.

Table 1. Clinical parameters of ART-treated PWH participants

ID	Sex	Ethnicity	Age&	CD4#	CD8 #	Plasma VL[a]	Time since infection[b]	ART regimen	Time on ART[b]
ART #1	M	Caucasian	36	542	803	<40	13	Stribild	12
ART #2	M	Caucasian	49	458	899	<40	201	Truvada Viramune	201
ART #3	M	Caucasian	58	546	1,116	<40	408	Atripla	369
ART #4	M	Caucasian	44	546	775	<40	154	Complera	25
ART #5	M	Caucasian	51	546	1,322	<40	149	Sustiva Truvada	149
ART #6	M	Caucasian	33	546	854	<40	89	Stribild	77
ART #7	M	Caucasian	21	546	399	<40	8	Stribild	4
ART #8	M	Caucasian	47	546	1,156	<40	182	Atripla	63
ART #9	M	Caucasian	59	546	836	<40	273	Symtuva	273
ART #10	M	Caucasian	64	546	620	<40	186	Triumeq	186
ART #11	M	Latino-American	31	546	1,000	<40	69	Complera	N/A
ART #12	M	Caucasian	30	546	605	<40	80	Stribild	77
ART #13	F	Caucasian	31	546	445	<40	212	Viracept Truvada	187

ID, participant identification code; ART, antiretroviral treated PWH; M, male; F, male; &, years; #, counts of cells/μL blood; N/A, not available.
[a]HIV-RNA copies per mL of plasma.
[b]Months.

Metformin increases intracellular Bcl-2 expression

We previously reported that 12 weeks of metformin treatment in complement of ART in PWH increased Bcl-2, an anti-apoptotic and pro-survival marker, in colon CCR6$^+$ CD4$^+$ T cells.[27] We therefore investigated whether metformin increases the frequency of productively HIV-infected T cells by promoting their survival in a Bcl-2-dependent manner. Memory CD4$^+$ T cells harvested at day 12 post-infection with HIV-1 $_{NL4.3Bal}$ *in vitro* were analyzed for intracellular Bcl-2 expression by flow cytometry on productively infected (CD4^{low}HIV-p24$^+$) versus uninfected (CD4^{high}HIV-p24$^-$) T cells (Figure 5A). Metformin, but not INK128, significantly increased the expression of Bcl-2 in both productively HIV-infected and uninfected CD4$^+$ T-cells (Figure 5B). These results suggest that metformin treatment promotes cell survival, in line with the use of metformin as a senolytic drug.[45]

Metformin facilitates recognition of reactivated VR by HIV-Env antibodies

To determine whether metformin may be used to accelerate VR decay in ART-treated PWH, we hypothesized that metformin increases the recognition of reactivated VR by HIV-1 envelope (Env) Abs, thus facilitating their purging via Abs-dependent mechanisms. To test this hypothesis, we performed a VOA, as described in Figure 3A. Cells harvested at day 12 post-TCR triggering in the presence or the absence of metformin were stained on the surface with CD4 Abs and a set of broadly neutralizing (bNAbs; 2G12, PGT121, PGT126, PGT151, 3BNC117, 101074, VRC03) and non-neutralizing (nnAbs; F240, 17b, A32) HIV-1 Env Abs, and with cell-associated HIV-p24 KC57 Abs (Figure 6A). The analysis was performed using a gating strategy depicted in Figure S5A. Different HIV-1 Env Abs showed a distinct ability to bind on productively infected cells (CD4^{low}HIV-p24$^+$) exposed or not to metformin (Figure 6A). Statistical analysis revealed that metformin increased the recognition of CD4^{low}HIV-p24$^+$ by the PGT126 bnAbs, in terms of frequency and mean fluorescence intensity (Figures 6B and 6C). PTG126 bnAbs recognizes the "*closed*" conformation of the HIV-1 Env (high-mannose patch on HIV gp120),[46] indicative that, upon TCR-mediated reactivation of VRs in ART-treated PWH, metformin increased the surface expression of HIV-1 Env in its "*closed*" conformation. Finally, considering the principle of HIV-Flow assay, where two distinct HIV-p24 Abs were used to specifically identify productively infected T cells,[47] further the frequency of CD4^{low} T cells co-expressing HIV-p24 and HIV-Env on CD4^{low} cells was analyzed within live cells (Figure S5B). Staining performed in parallel on cells from one HIV-uninfected donor showed low/undetectable levels of non-specific HIV-p24 and HIV-Env Ab binding (Figure S5C). Metformin significantly increased the frequency of T cells expressing HIV-p24 co-recognized by multiple HIV-Env Abs (i.e., PGT121, PGT126, PGT151, 101074, F240, A32) (Figure 6D). The dual staining with HIV-p24 and HIV-Env Abs likely represents a new strategy for the identification of VRs detectable by the immune system. Whether this recognition could translate in potential killing of infected cells by Ab-dependent cell toxicity (ADCC) remains to be determined.

DISCUSSION

Although ART has saved and substantially improved the life of PWH, the treatment is not curative and chronic HIV-1 infection is associated with several comorbidities that represent a global health burden.[1,8] New therapeutic strategies are needed to reduce chronic inflammation,

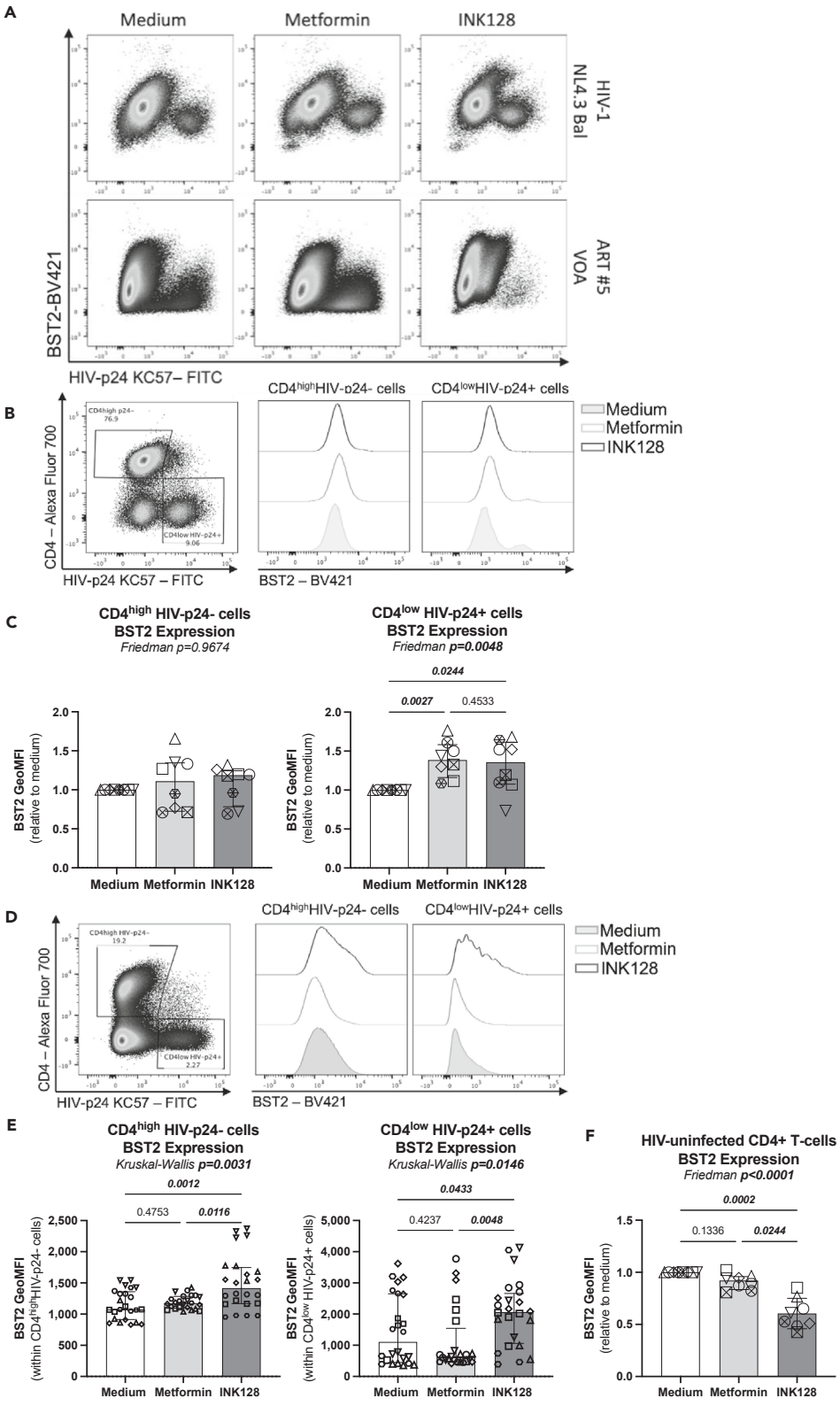
A
Medium
Metformin
INK128
HIV-1 NL4.3 Bal
ART #5 VOA
BST2-BV421
HIV-p24 KC57– FITC
B
CD4highHIV-p24- cells
CD4lowHIV-p24+ cells
Medium
Metformin
INK128
CD4 – Alexa Fluor 700
HIV-p24 KC57 – FITC
BST2 – BV421
C
CD4high HIV-p24- cells
BST2 Expression
Friedman p=0.9674
CD4low HIV-p24+ cells
BST2 Expression
Friedman p=0.0048
0.0244
0.0027
0.4533
BST2 GeoMFI
(relative to medium)
Medium Metformin INK128
D
CD4highHIV-p24- cells
CD4lowHIV-p24+ cells
Medium
Metformin
INK128
CD4 – Alexa Fluor 700
HIV-p24 KC57 – FITC
BST2 – BV421
E
CD4high HIV-p24- cells
BST2 Expression
Kruskal-Wallis p=0.0031
0.0012
0.4753
0.0116
BST2 GeoMFI
(within CD4highHIV-p24- cells)
CD4low HIV-p24+ cells
BST2 Expression
Kruskal-Wallis p=0.0146
0.0433
0.4237
0.0048
BST2 GeoMFI
(within CD4low HIV-p24+ cells)
Medium Metformin INK128
F
HIV-uninfected CD4+ T-cells
BST2 Expression
Friedman p<0.0001
0.0002
0.1336
0.0244
BST2 GeoMFI
(relative to medium)
Medium Metformin INK128

Figure 4. Metformin increases BST2 expression on productively infected CD4^{low}HIV-p24^{+} T cells

(A) Shown are representative flow cytometry dot plots of BST2 and HIV-p24 co-expression on T cells at day12 post-infection with HIV-1$_{NL4.3\ Bal}$ *in vitro* (upper panel) and at day 12 post TCR-mediated VR reactivation in VOA (bottom panel).

(B and C) The HIV-1$_{NL4.3Bal}$ infection *in vitro* was performed as described in Figure 3. Cells collected at day 12 post-infection were stained on the surface with CD4 and BST2 antibodies and with HIV-p24 antibodies and analyzed by flow cytometry for $n = 8$. Shown are (B) levels of BST2 expression on uninfected (CD4^{high}HIV-p24^{-}) and productively infected (CD4^{low}HIV-p24^{+}) T cells in one representative donor and (C) statistical analysis of BST2 expression (GeoMFI) relative to the medium condition (considered 1).

(D and E) The VOA was performed as described in Figure 1 with cells from $n = 6$ ART-treated PWH. Cells collected at day 12 post-stimulation were stained on the surface with CD4 and BST2 Abs and intracellularly with HIV-p24 Abs and analyzed by flow cytometry.

(D and E) Shown are levels of BST2 expression on CD4^{high}HIV-p24^{-} and CD4^{low}HIV-p24^{+} T cells in (D) one representative donor and (E) statistical analysis of BST2 expression (absolute GeoMFI).

(F) Shown is the BST2 expression relative to the medium condition of HIV-uninfected memory CD4^{+} T cells at day 3 post-TCR stimulation. Each symbol represents one donor (median ± interquartile range). Friedman (C and F), Kuskal-Wallis (E) and uncorrected Dunn's multiple comparison p values are indicated on the graphs.

improve immune functions, and accelerated the decay of VRs. HIV-1 infection modifies the metabolism of immune cells and thus, cellular metabolism could be a potential target for HIV-1 cure interventions.[48] By using metformin, an FDA approved anti-diabetic drug that reduces mTOR pathway activity,[25] we expected to reduce HIV-1 replication. Unexpectedly, metformin treatment increased the frequency of productively infected T cells in the context of a VOA performed with memory CD4^{+} T cells from ART-treated PWH, as well as upon HIV-1 infection *in vitro*. Nevertheless, the increase in the frequency of productively HIV-infected T cells did not lead to a proportional increase in progeny free-virion release. These effects were associated with increased expression of BST2 and/or Bcl-2 on productively infected T cells. Finally, the finding that metformin promotes the immune recognition by HIV-Env Abs (i.e., bnAbs PGT126) of T cells carrying translation-competent VRs emphasize the potential beneficial effect of metformin in accelerating the decay of VRs in ART-treated PWH in the context of efficient HIV-Env Abs-mediated antiviral responses, such as ADCC.[49]

In this study, we used three viral models that allowed us to dissect specific steps of the viral replication cycle affected by metformin. In the VOA, the outgrowth of replication-competent virions was quantified in memory CD4^{+} T cells of ART-treated PWH upon culture *in vitro*, with the genetic features of VR proviruses (mutations, deletions) remaining unknown. For *in vitro* infections, we used the HIV$_{NL4.3BaL}$ molecular clone, a wild-type replication-competent CCR5-tropic HIV-1, and the single-round HIV$_{VSV-G}$ construct contained an EGFP gene inserted in the Env gene, leading to the generation of Env-defective HIV-1 virions. In all three models, metformin treatment did not increase viral release but increased the frequency of productively infected CD4^{low}HIV-p24^{+} T cells. Mechanisms by which metformin increased the frequency of productively HIV-infected cells, without a proportional viral release in all three viral model remains to be evaluated. In the replication competent HIV$_{NL4.3BaL}$ infection *in vitro*, metformin increased cell-associated HIV-p24, decreased free-virion release, and prevented the HIV-induced downregulation of BST2, a phenomenon that we did not observe in the two other experimental models. Metformin effects were less pronounced in experiments performed with HIV$_{VSV-G}$, in line with the inability of Env-defective viruses to be tethered at the cell-surface via BST2 and to infect new cells. Infection using a single round VSVG pseudotyped HIV virus showed that metformin acts on the post-integration steps of the HIV replication cycle, such as translation, assembly, budding, and/or free-virion release. HIV transcription was not evaluated in the current studies. Metformin effects in VOA were abrogated by ARVs, further supporting the idea of a metformin-mediated mechanism of cell-to-cell transmission independent of free-virion release. These findings suggest that metformin facilitates the reactivation of VR cells.

mTOR controls Th17 polarization and functions.[50,51] Direct mTOR inhibitors such as INK128 and rapamycin reduce IL-17A production.[52,53] Metformin was previously reported to reduce IL-17A production and RORC2 expression *in vitro*.[54] The latter report contrasts with results from our study, likely because the latter study was performed under Th17-polarizing conditions. Our results show that metformin treatment, in contrast to INK128, promotes CCR6 and RORC2 protein expression and maintains the Th17 cell effector functions (i.e., IL-17A). Th17 cells are largely depleted after HIV-1 infection and their maintenance is linked to a better control of HIV-1 replication in elite controller.[53,55] Furthermore, studies by our group demonstrated that Th17 cells are highly susceptible to HIV-1 infection given their unique high metabolic activity and transcriptional profiles.[20,35,36,56,57] The pleiotropic effects of metformin on various steps of the viral replication cycle coincided with an increased Th17-polarization phenotype (CCR6^{+}RORC2^{+}), and a preserved IL-17A production. Therefore, metformin treatment could exert its proviral activities by boosting Th17 polarization.

Another major finding of our study is the demonstration that metformin increased the expression of BST2, a host-cell restriction factor originally reported to tether progeny virions on the cell surface, thus preventing their release.[42] Further studies reported that basal levels of BST2-mediated virion tethering are required for efficient cell-to-cell transmission of HIV-1,[40] mainly in primary cells.[58] Indeed, we found that, upon HIV-1 exposure *in vitro*, metformin reduced cell-free virion levels, while enhancing the frequency of productively infected cells and boosting their BST2 expression. In contrast to metformin, INK128 decreased cell-surface BST2 expression. Considering that BST2 is a viral restriction factor induced by type I interferon[41] and that mTOR activation induces interferon production,[59] we hypothesized that INK128-mediated mTOR blockade reduced BST2 expression in an interferon-dependent manner. The antiviral features of BST2 are regulated via glycosylation, intracellular trafficking and epigenetic modifications.[60–62] BST2 exists in two isoforms, long (L-tetherin) and short (S-tetherin), with Vpu mainly targeting the long isoforms.[63] The fact that BST2 acts through an interaction with the HIV-1 Env,[42,64] explains the accumulation of cell-associated HIV-p24 in T cells upon exposure to wild type HIV$_{NL4.3\ Bal}$ but not Env-deficient VSVG-pseudotyped HIV-1. The HIV-1 accessory protein Vpu facilitates viral release by decreasing BST2 expression and its restriction activity,[42] pointing to the possibility that metformin counteracts the Vpu-mediated BST2 downregulation on infected T cells. The ability of Vpu to counteract BST2 depends on its serine

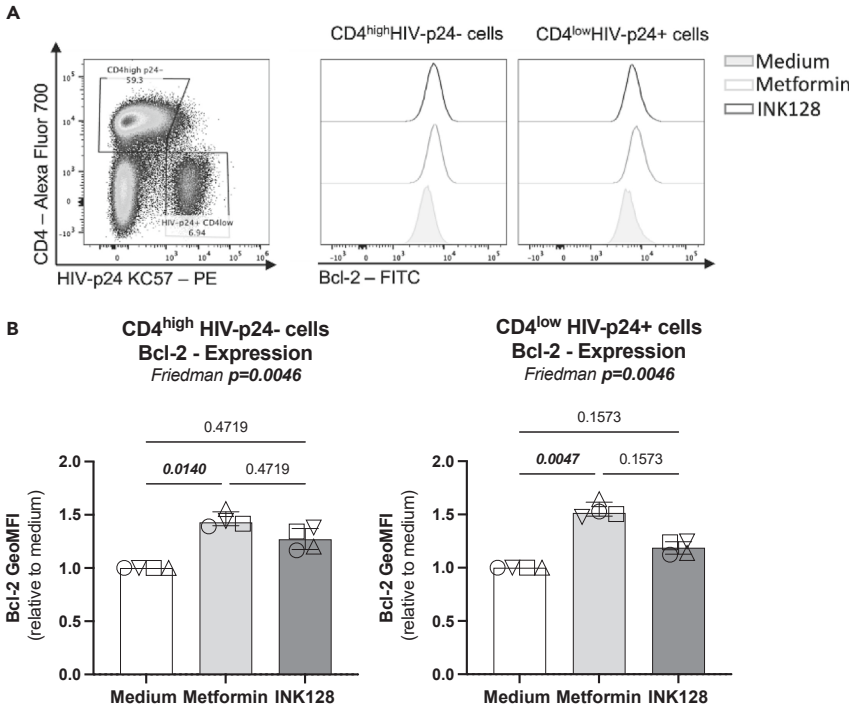

Figure 5. Metformin increases Bcl-2 expression on HIV-infected and uninfected T cells

The HIV-$1_{NL4.3Bal}$ infection *in vitro* was performed as described in Figure 3. Cells collected at day 12 post-infection were stained with CD4, HIV-p24, and Bcl-2antibodies and analyzed by flow cytometry. Shown are (A) levels of Bcl-2 expression on uninfected ($CD4^{high}HIV\text{-}p24^{-}$) and productively infected ($CD4^{low}HIV\text{-}p24^{+}$) T cells in one representative donor and (B) statistical analysis of Bcl-2 expression (GeoMFI) relative to the medium condition (considered 1). Each symbol represents one donor ($n = 4$; median ± interquartile range). Friedman and uncorrected Dunn's multiple comparison p values are indicated on the graphs.

phosphorylation,[65] a process that may be modulated by metformin in a mTOR-dependent manner. Additionally, activation of the PI3K signaling pathway, which acts upstream to activate the mTOR pathway, results in reduced cell-surface expression of BST2 in macrophages,[66] thereby suggesting a potential role of metformin in regulating BST2 expression via a mTOR-dependent mechanism. In VOA, BST2 expression on productively infected cells was not influenced by metformin, consistent with the fact that a metformin-mediated increase in cell-associated HIV-p24 expression was not observed at single cell level in the VOA. This raises new questions on the specificity of metformin action in relationship with the particularities of reactivated proviruses. Molecular mechanisms by which metformin regulate BST2 expression and functions (e.g., transcription of specific isoforms, glycosylation, cellular localization, modulation of Vpu expression, epigenetic modifications) remain to be further elucidated.

The effects of metformin on the expansion of productively infected T cells upon infection *in vitro* were also associated with an increased expression of Bcl-2, a mitochondrial protein associated with cell survival.[67] The upregulation of Bcl-2 by metformin on colon-infiltrating $CCR6^{+}CD4^{+}$ T cells was also observed in our LILAC pilot clinical trial.[27] Most recent studies demonstrated the clinical benefits of Bcl-2 inhibitors (i.e., Venetoclax) in promoting VR purging.[68–71] Whether metformin supplementation of ART may render reactivated VR more sensitive to Bcl-2 blockade, requires investigations in *in vivo* models.

In HIV eradication strategies, both the "*shock*" and "*kill*" arms will be required.[72,73] BST2 acts as an innate sensor of viral assembly,[74] suggesting that metformin may facilitate VR sensing by the immune system via BST2-dependent mechanisms. Indeed, studies by our group and others documented the ability of BST2 to facilitate ADCC.[75–80] In this context, we assessed the impact of metformin on the recognition of reactivated VRs by bNAbs and nnAbs. We demonstrated that metformin treatment increased the frequency of productively infected $CD4^{+}$ T cells recognized by the bNAbs PGT126, as well as its binding intensity at the single-cell level. The antiviral activities of PGT126 bNAbs were tested in a rhesus macaque infection model, in which PGT126 Abs administered before vaginal or rectal SHIV challenge displayed protective effects against infection acquisition.[76,81] Whether metformin can increase the ADCC activity of PGT126 Abs for infected cells remains to be demonstrated. If so, a combination therapy including metformin and bNAbs could be beneficial to reduce the size of HIV-1 reservoirs during ART. In addition to ADCC mediated by NK cells, $CD8^{+}$ T cells are also key effectors for the control HIV-1 replication.[82,83] Of interest, $CD8^{+}$ T cells differentiation and antiviral functions are dependent on the mTOR activity.[84] In this context, the role of metformin treatment on $CD8^{+}$ T cell-mediated killing of HIV-infected T cells remain to be elucidated. In line with this possibility, studies in tumor cell lines demonstrated that metformin increased the cytotoxic activities of $CD8^{+}$ T cells against cancerous cells.[85] Of note, eight weeks of metformin treatment in nondiabetic PWH increased the cytotoxic response of $CD8^{+}$ T cells.[86] These data support the idea that metformin could have a beneficial effect both on HIV-1 reservoir reactivation and on the quality of HIV-specific $CD8^{+}$ T cell responses.

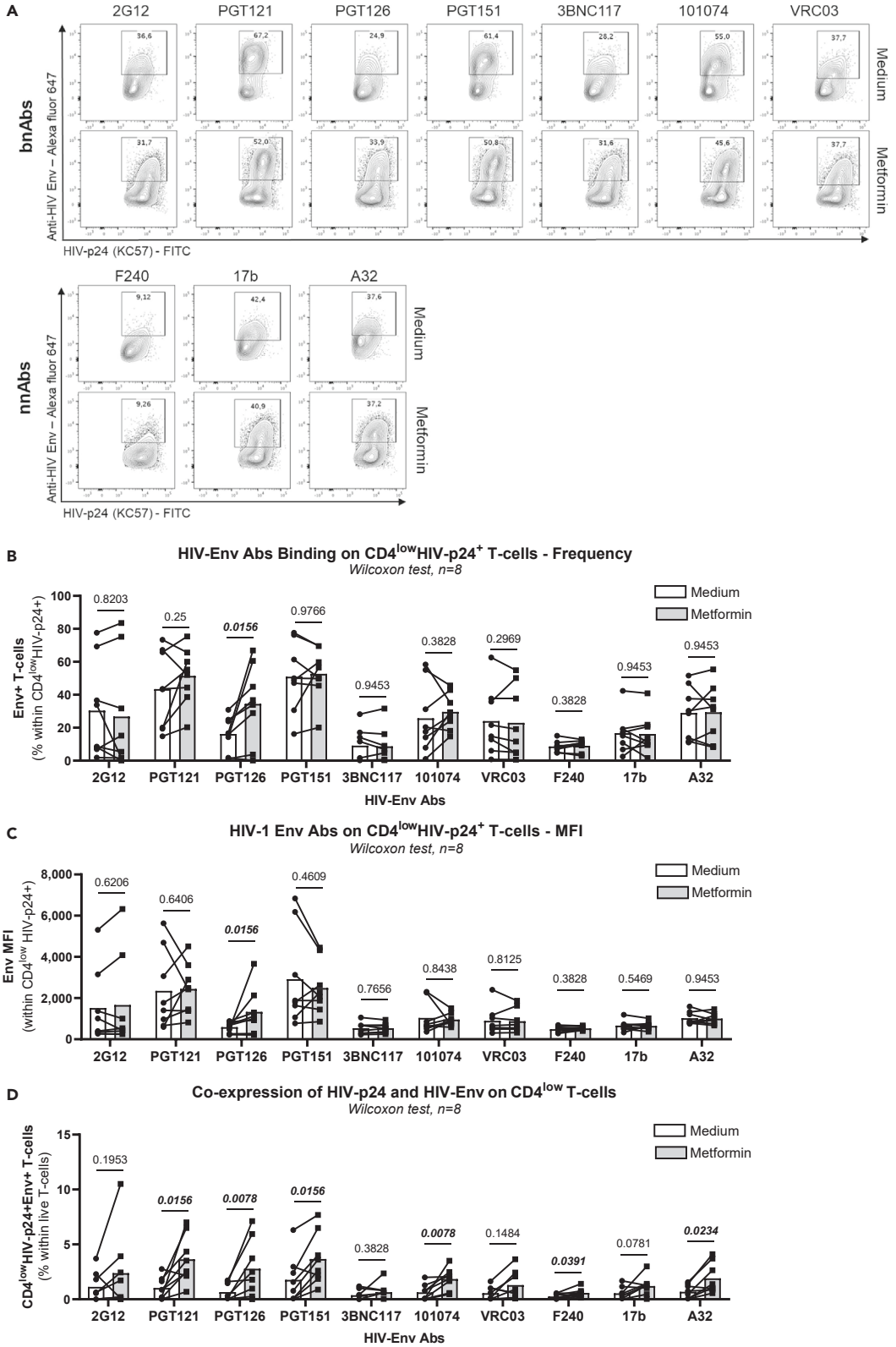
A
2G12
PGT121
PGT126
PGT151
3BNC117
101074
VRC03
bnAbs
Anti-HIV Env – Alexa fluor 647
HIV-p24 (KC57) - FITC
Medium
Metformin
F240
17b
A32
nnAbs
B
HIV-Env Abs Binding on CD4lowHIV-p24+ T-cells - Frequency
Wilcoxon test, n=8
Env+ T-cells
(% within CD4lowHIV-p24+)
HIV-Env Abs
C
HIV-1 Env Abs on CD4lowHIV-p24+ T-cells - MFI
Wilcoxon test, n=8
Env MFI
(within CD4low HIV-p24+)
D
Co-expression of HIV-p24 and HIV-Env on CD4low T-cells
Wilcoxon test, n=8
CD4lowHIV-p24+Env+ T-cells
(% within live T-cells)

Figure 6. Metformin facilitates the recognition of reactivated HIV reservoirs by anti-HIV Env antibodies

The VOA was performed on memory CD4$^+$ T cells from ART-treated PWH, as described in Figure 3A. Cells harvested at day 12 post-TCR triggering and cultured in the presence/absence of metformin (1 mM) were stained on the surface with a set of unconjugated human anti-HIV-1 Env bNAbs (2G12, PGT121, PGT126, PGT151, 3BNC117, 101074, VRC03) and nnAbs (F240, 17b, A32), followed by incubation with anti-human Alexa Fluor 647-conjugated secondary Abs. Further, cells were stained on the surface with CD4 Abs, as well as intracellularly with HIV-p24 Abs. (A) Show are flow cytometry dot plot representations of HIV-Env Ab binding on productively infected CD4^{low}HIV-p24$^+$ T-cells in one representative donor, gated as depicted in Figure S5A. Statistical analysis were performed to determine the effect of metformin on the frequency of CD4^{low}HIV-p24$^+$ T cells recognized by anti-HIV-Env Abs (B), as well as the geometric MFI of HIV-Env expression (C). Finally, statistical analysis were performed to determine the effect of metformin on the frequency of T cells co-expressing cell-associated HIV-p24 and surface HIV-Env (D), gated as in Figures S5A and S5B. Wilcoxon test *p* values are indicated on the graphs. Each symbol represents one donor (n = 8; median ± interquartile range).

In conclusion, our results support a model in which metformin supplementation of ART facilitates the expression of HIV-p24, helps tether the progeny virions on the cell surface via a BST2 dependent mechanism and promote their enhanced recognition by HIV-1 Env bnNAbs (i.e., PGT126). Considering its pleiotropic pro/antiviral effects on specific steps of the HIV-1 replication cycle, long-term double blind clinical trials should be performed to test metformin together with HIV-1 Env bNAbs in complement of ART in PWH as a novel HIV-1 remission/cure strategy to target HIV reservoirs.

Limitations of the study

Although the optimal metformin concentrations used in our *in vitro* study (1 mM) were identified based on dose-response testing, it may not reflect the actual concentration in tissues upon metformin administration in clinic.[27] Since metformin, taken orally, mostly acts in tissues such as the intestines and liver, we cannot guarantee that the effects observed *in vitro* on peripheral blood CD4$^+$ T cells may be consistent with the reality *in vivo*. However, our decision to use metformin at 1 mM is justified by its effect on mTOR activation and HIV-1 replication, without affecting cell viability and proliferation (Figure 1; Figure S1). Also, studies by other groups also reported results using the same concentration of metformin *in vitro*.[28,54] To decipher the molecular mechanisms used by metformin to reactivate HIV-1 reservoirs in VOA, the step of HIV transcription requires detailed investigations. Future studies on T cells enriched in VRs, such as CCR6+ Th17 cells,[36,37] may be required for an accurate monitoring of metformin effect on HIV transcription. Also, chromatin immunoprecipitation (ChIP) and quantitative PCR (qPCR) studies should investigate the effect of metformin on the recruitment of transcription factors and cofactors to the HIV promoter, using approaches we recently reported.[87] The flow cytometry staining of cell-associated HIV-p24 did not allow to distinguish whether virions were trapped in the cytoplasm, at the inner or at the outer cell surface membrane. Further investigation using microscopy visualization should be performed.

Finally, our studies were mainly performed on cells from Caucasian male participants with HIV-1 clade B infection (i.e., 1 female, 12 males; 1 Latin-American, 12 Caucasians). Differences linked to sex, gender, ethnicity, and HIV clade could have an impact on the effect of metformin treatment. Indeed, non-AIDS comorbidities and metabolic disorders vary depending on sex and ethnicity.[88] These aspects should be further investigated in an effort to implement precision medicine strategies.

STAR★METHODS

Detailed methods are provided in the online version of this paper and include the following:

- KEY RESOURCES TABLE
- RESOURCE AVAILABILITY
  - Lead contact
  - Materials availability
  - Data and code availability
  - Ethics statement
  - Study participants
  - Memory CD4$^+$ T cell sorting
  - Flow cytometry analysis
  - Cell culture and activation
  - Compounds
  - HIV viral stocks
  - HIV-1 infection *in vitro*
  - Viral Outgrowth Assay (VOA)
  - Quantification of early, late reverse transcript and integrated HIV-DNA
  - Anti-HIV-1 envelope antibodies recognition of productively HIV-infected T-cells
  - HIV-1 env antibody production
  - Western blot
- STATISTICAL ANALYSIS

SUPPLEMENTAL INFORMATION

Supplemental information can be found online at https://doi.org/10.1016/j.isci.2024.110670.

ACKNOWLEDGMENTS

We thank Dr. Dominique Gauchat, Philippe St Onge, and Gaël Dulude (Flow Cytometry Core Facility, CHUM-Research Center, Montréal, QC, Canada) for expert technical support; Olfa Debbeche and Laurent Knafo (Biosafety Level 3 Core Facility CHUM-Research Center). We acknowledge the key contribution of all study participants for their precious gift of leukapheresis. We thank the following collaborators for kindly providing plasmids to produce antibodies: James Robinson (Tulane University) for A32; John Mascola (Vaccine Research Center, NIAID) for VRC03; Michel Nussenzweig for 3BNC117 and 10–1074; the NIH AIDS Reagent Program for F240, 2G12, and 17b; and the International AIDS Vaccine Initiative (IAVI) for PGT121, PGT126, PGT151. The authors thank Jonathan Dias for assistance with manuscript editing.

This study was funded by grants from the Canadian Institutes of Health Research (CIHR; PJT-153052; PJT-178127 to P.A.), the Canadian HIV Cure Enterprise Team grant (CanCURE 1.0) funded by CIHR in partnership with the Canadian Foundation for AIDS Research and the International AIDS Society (CanCURE 1.0; HIG-133050 to P.A.), and the CanCURE 2.0 Team grant funded by CIHR (HB2-164064 to P.A.). This work was also supported by grants from the National Institutes of Health (NIH; R01 AI148379; R01 AI150322), a CIHR team grant [422148] and the Enterprise for Research and Advocacy to Stop and Eradicate HIV (ERASE, UM1AI164562) to A.Fi. and the Delaney AIDS Research Enterprise to Cure HIV (DARE, UM1AI164560) to A.Fi. and N.C. A.Fi. is the recipient of a Canada Research Chair on Retroviral Entry [RCHS0235 950-232424]. A.Fe. and D.P. received doctoral fellowship from the Université de Montréal and Fonds de Recherche Québec - Santé (FRQ-S). Core facilities and PWH cohorts were supported by the *Fondation du CHUM* and the FRQ-S/AIDS and Infectious Diseases Network. The funding institutions played no role in the design, collection, analysis, and interpretation of data.

AUTHOR CONTRIBUTIONS

Conceptualization, A.Fe., D.P., and P.A.; methodology, A.Fe., D.P., P.A., J.R., and A.Fi.; investigation and formal analysis, A.Fe., J.R., and L.R.M.; resources, J.-P.R., N.C., P.A., and A.Fi.; writing – original draft, A.Fe.; writing – review & editing, A.Fe., D.P., J.R., A.Fi., N.C., L.R.M., J.-P.R., and P.A.; supervision, A.Fi., N.C., and P.A.; funding acquisition, P.A.,; project administration, P.A.

DECLARATION OF INTERESTS

The authors declare no competing interests.

Received: February 13, 2024
Revised: May 27, 2024
Accepted: August 1, 2024
Published: August 5, 2024

REFERENCES

1. Bai, R.J., Dai, L.L., and Wu, H. (2020). Advances and challenges in antiretroviral therapy for acquired immunodeficiency syndrome. Chin. Med. J. *133*, 2775–2777. https://doi.org/10.1097/CM9.0000000000001226.
2. Hsue, P.Y., and Waters, D.D. (2018). Time to Recognize HIV Infection as a Major Cardiovascular Risk Factor. Circulation *138*, 1113–1115. https://doi.org/10.1161/CIRCULATIONAHA.118.036211.
3. Wang, C.C.J., Silverberg, M.J., and Abrams, D.I. (2014). Non-AIDS-Defining Malignancies in the HIV-Infected Population. Curr. Infect. Dis. Rep. *16*, 406. https://doi.org/10.1007/s11908-014-0406-0.
4. Samaras, K., Wand, H., Law, M., Emery, S., Cooper, D., and Carr, A. (2007). Prevalence of metabolic syndrome in HIV-infected patients receiving highly active antiretroviral therapy using International Diabetes Foundation and Adult Treatment Panel III criteria: associations with insulin resistance, disturbed body fat compartmentalization, elevated C-reactive protein, and [corrected] hypoadiponectinemia. Diabetes Care *30*, 113–119. https://doi.org/10.2337/dc06-1075.
5. Akusjarvi, S.S., and Neogi, U. (2023). Biological Aging in People Living with HIV on Successful Antiretroviral Therapy: Do They Age Faster? Curr. HIV AIDS Rep. *20*, 42–50. https://doi.org/10.1007/s11904-023-00646-0.
6. Desquilbet, L., Jacobson, L.P., Fried, L.P., Phair, J.P., Jamieson, B.D., Holloway, M., and Margolick, J.B.; Multicenter AIDS Cohort Study (2007). HIV-1 infection is associated with an earlier occurrence of a phenotype related to frailty. J. Gerontol. A Biol. Sci. Med. Sci. *62*, 1279–1286. https://doi.org/10.1093/gerona/62.11.1279.
7. Massanella, M., Fromentin, R., and Chomont, N. (2016). Residual inflammation and viral reservoirs: alliance against an HIV cure. Curr. Opin. HIV AIDS *11*, 234–241. https://doi.org/10.1097/COH.0000000000000230.
8. Deeks, S.G., and Phillips, A.N. (2009). HIV infection, antiretroviral treatment, ageing, and non-AIDS related morbidity. BMJ *338*, a3172. https://doi.org/10.1136/bmj.a3172.
9. Fletcher, C.V., Staskus, K., Wietgrefe, S.W., Rothenberger, M., Reilly, C., Chipman, J.G., Beilman, G.J., Khoruts, A., Thorkelson, A., Schmidt, T.E., et al. (2014). Persistent HIV-1 replication is associated with lower antiretroviral drug concentrations in lymphatic tissues. Proc. Natl. Acad. Sci. USA *111*, 2307–2312. https://doi.org/10.1073/pnas.1318249111.
10. Mehandru, S., Poles, M.A., Tenner-Racz, K., Jean-Pierre, P., Manuelli, V., Lopez, P., Shet, A., Low, A., Mohri, H., Boden, D., et al. (2006). Lack of mucosal immune reconstitution during prolonged treatment of acute and early HIV-1 infection. PLoS Med. *3*, e484. https://doi.org/10.1371/journal.pmed.0030484.
11. Martinez-Picado, J., and Deeks, S.G. (2016). Persistent HIV-1 replication during antiretroviral therapy. Curr. Opin. HIV AIDS *11*, 417–423. https://doi.org/10.1097/COH.0000000000000287.
12. Guadalupe, M., Reay, E., Sankaran, S., Prindiville, T., Flamm, J., McNeil, A., and Dandekar, S. (2003). Severe CD4+ T-cell depletion in gut lymphoid tissue during primary human immunodeficiency virus type 1 infection and substantial delay in restoration following highly active antiretroviral therapy. J. Virol. *77*, 11708–11717. https://doi.org/10.1128/jvi.77.21.11708-11717.2003.
13. Saxton, R.A., and Sabatini, D.M. (2017). mTOR Signaling in Growth, Metabolism, and Disease. Cell *168*, 960–976. https://doi.org/10.1016/j.cell.2017.02.004.
14. Chi, H. (2012). Regulation and function of mTOR signalling in T cell fate decisions. Nat.

Rev. Immunol. *12*, 325–338. https://doi.org/10.1038/nri3198.
15. Heredia, A., Le, N., Gartenhaus, R.B., Sausville, E., Medina-Moreno, S., Zapata, J.C., Davis, C., Gallo, R.C., and Redfield, R.R. (2015). Targeting of mTOR catalytic site inhibits multiple steps of the HIV-1 lifecycle and suppresses HIV-1 viremia in humanized mice. Proc. Natl. Acad. Sci. USA *112*, 9412–9417. https://doi.org/10.1073/pnas.1511144112.
16. Clerc, I., Moussa, D.A., Vahlas, Z., Tardito, S., Oburoglu, L., Hope, T.J., Sitbon, M., Dardalhon, V., Mongellaz, C., and Taylor, N. (2019). Entry of glucose- and glutamine-derived carbons into the citric acid cycle supports early steps of HIV-1 infection in CD4 T cells. Nat. Metab. *1*, 717–730. https://doi.org/10.1038/s42255-019-0084-1.
17. Besnard, E., Hakre, S., Kampmann, M., Lim, H.W., Hosmane, N.N., Martin, A., Bassik, M.C., Verschueren, E., Battivelli, E., Chan, J., et al. (2016). The mTOR Complex Controls HIV Latency. Cell Host Microbe *20*, 785–797. https://doi.org/10.1016/j.chom.2016.11.001.
18. Taylor, H.E., Calantone, N., Lichon, D., Hudson, H., Clerc, I., Campbell, E.M., and D'Aquila, R.T. (2020). mTOR Overcomes Multiple Metabolic Restrictions to Enable HIV-1 Reverse Transcription and Intracellular Transport. Cell Rep. *31*, 107810. https://doi.org/10.1016/j.celrep.2020.107810.
19. Finkelshtein, D., Werman, A., Novick, D., Barak, S., and Rubinstein, M. (2013). LDL receptor and its family members serve as the cellular receptors for vesicular stomatitis virus. Proc. Natl. Acad. Sci. USA *110*, 7306–7311. https://doi.org/10.1073/pnas.1214441110.
20. Planas, D., Zhang, Y., Monteiro, P., Goulet, J.P., Gosselin, A., Grandvaux, N., Hope, T.J., Fassati, A., Routy, J.P., and Ancuta, P. (2017). HIV-1 selectively targets gut-homing CCR6+CD4+ T cells via mTOR-dependent mechanisms. JCI Insight *2*, e93230. https://doi.org/10.1172/jci.insight.93230.
21. Tedesco-Silva, H., Saliba, F., Barten, M.J., De Simone, P., Potena, L., Gottlieb, J., Gawai, A., Bernhardt, P., and Pascual, J. (2022). An overview of the efficacy and safety of everolimus in adult solid organ transplant recipients. Transplant. Rev. *36*, 100655. https://doi.org/10.1016/j.trre.2021.100655.
22. Henrich, T.J., Schreiner, C., Cameron, C., Hogan, L.E., Richardson, B., Rutishauser, R.L., Deitchman, A.N., Chu, S., Rogers, R., Thanh, C., et al. (2021). Everolimus, an mTORC1/2 inhibitor, in ART-suppressed individuals who received solid organ transplantation: A prospective study. Am. J. Transplant. *21*, 1765–1779. https://doi.org/10.1111/ajt.16244.
23. Lv, Z., and Guo, Y. (2020). Metformin and Its Benefits for Various Diseases. Front. Endocrinol. *11*, 191. https://doi.org/10.3389/fendo.2020.00191.
24. Howell, J.J., Hellberg, K., Turner, M., Talbott, G., Kolar, M.J., Ross, D.S., Hoxhaj, G., Saghatelian, A., Shaw, R.J., and Manning, B.D. (2017). Metformin Inhibits Hepatic mTORC1 Signaling via Dose-Dependent Mechanisms Involving AMPK and the TSC Complex. Cell Metab. *25*, 463–471. https://doi.org/10.1016/j.cmet.2016.12.009.
25. Pernicova, I., and Korbonits, M. (2014). Metformin–mode of action and clinical implications for diabetes and cancer. Nat. Rev. Endocrinol. *10*, 143–156. https://doi.org/10.1038/nrendo.2013.256.
26. Routy, J.P., Isnard, S., Mehraj, V., Ostrowski, M., Chomont, N., Ancuta, P., Ponte, R., Planas, D., Dupuy, F.P., and Angel, J.B.; Lilac Study Group (2019). Effect of metformin on the size of the HIV reservoir in non-diabetic ART-treated individuals: single-arm non-randomised Lilac pilot study protocol. BMJ Open *9*, e028444. https://doi.org/10.1136/bmjopen-2018-028444.
27. Planas, D., Pagliuzza, A., Ponte, R., Fert, A., Marchand, L.R., Massanella, M., Gosselin, A., Mehraj, V., Dupuy, F.P., Isnard, S., et al. (2021). LILAC pilot study: Effects of metformin on mTOR activation and HIV reservoir persistence during antiretroviral therapy. EBioMedicine *65*, 103270. https://doi.org/10.1016/j.ebiom.2021.103270.
28. Guo, H., Wang, Q., Ghneim, K., Wang, L., Rampanelli, E., Holley-Guthrie, E., Cheng, L., Garrido, C., Margolis, D.M., Eller, L.A., et al. (2021). Multi-omics analyses reveal that HIV-1 alters CD4(+) T cell immunometabolism to fuel virus replication. Nat. Immunol. *22*, 423–433. https://doi.org/10.1038/s41590-021-00898-1.
29. Shikuma, C.M., Chew, G.M., Kohorn, L., Souza, S.A., Chow, D., SahBandar, I.N., Park, E.Y., Hanks, N., Gangcuangco, L.M.A., Gerschenson, M., and Ndhlovu, L.C. (2020). Short Communication: Metformin Reduces CD4 T Cell Exhaustion in HIV-Infected Adults on Suppressive Antiretroviral Therapy. AIDS Res. Hum. Retroviruses *36*, 303–305. https://doi.org/10.1089/AID.2019.0078.
30. Fromentin, R., Bakeman, W., Lawani, M.B., Khoury, G., Hartogensis, W., DaFonseca, S., Killian, M., Epling, L., Hoh, R., Sinclair, E., et al. (2016). CD4+ T Cells Expressing PD-1, TIGIT and LAG-3 Contribute to HIV Persistence during ART. PLoS Pathog. *12*, e1005761. https://doi.org/10.1371/journal.ppat.1005761.
31. Isnard, S., Lin, J., Fombuena, B., Ouyang, J., Varin, T.V., Richard, C., Marette, A., Ramendra, R., Planas, D., Raymond Marchand, L., et al. (2020). Repurposing Metformin in Nondiabetic People With HIV: Influence on Weight and Gut Microbiota. Open Forum Infect. Dis. *7*, ofaa338. https://doi.org/10.1093/ofid/ofaa338.
32. Schenone, S., Brullo, C., Musumeci, F., Radi, M., and Botta, M. (2011). ATP-competitive inhibitors of mTOR: an update. Curr. Med. Chem. *18*, 2995–3014. https://doi.org/10.2174/092986711796391651.
33. Richard, J., Prévost, J., Baxter, A.E., von Bredow, B., Ding, S., Medjahed, H., Delgado, G.G., Brassard, N., Sturzel, C.M., Kirchhoff, F., et al. (2018). Uninfected Bystander Cells Impact the Measurement of HIV-Specific Antibody-Dependent Cellular Cytotoxicity Responses. mBio *9*, 10–1128. https://doi.org/10.1128/mBio.00358-18.
34. Rhee, S.S., and Marsh, J.W. (1994). Human immunodeficiency virus type 1 Nef-induced down-modulation of CD4 is due to rapid internalization and degradation of surface CD4. J. Virol. *68*, 5156–5163. https://doi.org/10.1128/JVI.68.8.5156-5163.1994.
35. Fert, A., Raymond Marchand, L., Wiche Salinas, T.R., and Ancuta, P. (2022). Targeting Th17 cells in HIV-1 remission/cure interventions. Trends Immunol. *43*, 580–594. https://doi.org/10.1016/j.it.2022.04.013.
36. Monteiro, P., Gosselin, A., Wacleche, V.S., El-Far, M., Said, E.A., Kared, H., Grandvaux, N., Boulassel, M.R., Routy, J.P., and Ancuta, P. (2011). Memory CCR6+CD4+ T cells are preferential targets for productive HIV type 1 infection regardless of their expression of integrin beta7. J. Immunol. *186*, 4618–4630. https://doi.org/10.4049/jimmunol.1004151.
37. Gosselin, A., Wiche Salinas, T.R., Planas, D., Wacleche, V.S., Zhang, Y., Fromentin, R., Chomont, N., Cohen, É.A., Shacklett, B., Mehraj, V., et al. (2017). HIV persists in CCR6+CD4+ T cells from colon and blood during antiretroviral therapy. AIDS *31*, 35–48. https://doi.org/10.1097/QAD.0000000000001309.
38. Zhang, Y., Planas, D., Raymond Marchand, L., Massanella, M., Chen, H., Wacleche, V.S., Gosselin, A., Goulet, J.P., Filion, M., Routy, J.P., et al. (2020). Improving HIV Outgrowth by Optimizing Cell-Culture Conditions and Supplementing With *all-trans* Retinoic Acid. Front. Microbiol. *11*, 902. https://doi.org/10.3389/fmicb.2020.00902.
39. Jolly, C., Booth, N.J., and Neil, S.J.D. (2010). Cell-cell spread of human immunodeficiency virus type 1 overcomes tetherin/BST-2-mediated restriction in T cells. J. Virol. *84*, 12185–12199. https://doi.org/10.1128/JVI.01447-10.
40. Andrew, A., and Strebel, K. (2011). The interferon-inducible host factor bone marrow stromal antigen 2/tetherin restricts virion release, but is it actually a viral restriction factor? J. Interferon Cytokine Res. *31*, 137–144. https://doi.org/10.1089/jir.2010.0108.
41. Van Damme, N., Goff, D., Katsura, C., Jorgenson, R.L., Mitchell, R., Johnson, M.C., Stephens, E.B., and Guatelli, J. (2008). The interferon-induced protein BST-2 restricts HIV-1 release and is downregulated from the cell surface by the viral Vpu protein. Cell Host Microbe *3*, 245–252. https://doi.org/10.1016/j.chom.2008.03.001.
42. Neil, S.J.D., Zang, T., and Bieniasz, P.D. (2008). Tetherin inhibits retrovirus release and is antagonized by HIV-1 Vpu. Nature *451*, 425–430. https://doi.org/10.1038/nature06553.
43. Perez-Caballero, D., Zang, T., Ebrahimi, A., McNatt, M.W., Gregory, D.A., Johnson, M.C., and Bieniasz, P.D. (2009). Tetherin inhibits HIV-1 release by directly tethering virions to cells. Cell *139*, 499–511. https://doi.org/10.1016/j.cell.2009.08.039.
44. McNatt, M.W., Zang, T., and Bieniasz, P.D. (2013). Vpu binds directly to tetherin and displaces it from nascent virions. PLoS Pathog. *9*, e1003299. https://doi.org/10.1371/journal.ppat.1003299.
45. Kulkarni, A.S., Gubbi, S., and Barzilai, N. (2020). Benefits of Metformin in Attenuating the Hallmarks of Aging. Cell Metab. *32*, 15–30. https://doi.org/10.1016/j.cmet.2020.04.001.
46. Walker, L.M., Huber, M., Doores, K.J., Falkowska, E., Pejchal, R., Julien, J.P., Wang, S.K., Ramos, A., Chan-Hui, P.Y., Moyle, M., et al. (2011). Broad neutralization coverage of HIV by multiple highly potent antibodies. Nature *477*, 466–470. https://doi.org/10.1038/nature10373.
47. Pardons, M., Baxter, A.E., Massanella, M., Pagliuzza, A., Fromentin, R., Dufour, C., Leyre, L., Routy, J.P., Kaufmann, D.E., and Chomont, N. (2019). Single-cell characterization and quantification of translation-competent viral reservoirs in treated and untreated HIV infection. PLoS Pathog. *15*, e1007619. https://doi.org/10.1371/journal.ppat.1007619.
48. Saez-Cirion, A., and Sereti, I. (2021). Immunometabolism and HIV-1 pathogenesis: food for thought. Nat. Rev. Immunol. *21*,

5–19. https://doi.org/10.1038/s41577-020-0381-7.
49. Forthal, D.N., and Finzi, A. (2018). Antibody-dependent cellular cytotoxicity in HIV infection. AIDS *32*, 2439–2451. https://doi.org/10.1097/QAD.0000000000002011.
50. Delgoffe, G.M., Kole, T.P., Zheng, Y., Zarek, P.E., Matthews, K.L., Xiao, B., Worley, P.F., Kozma, S.C., and Powell, J.D. (2009). The mTOR kinase differentially regulates effector and regulatory T cell lineage commitment. Immunity *30*, 832–844. https://doi.org/10.1016/j.immuni.2009.04.014.
51. Shen, H., and Shi, L.Z. (2019). Metabolic regulation of T(H)17 cells. Mol. Immunol. *109*, 81–87. https://doi.org/10.1016/j.molimm.2019.03.005.
52. Kopf, H., de la Rosa, G.M., Howard, O.M.Z., and Chen, X. (2007). Rapamycin inhibits differentiation of Th17 cells and promotes generation of FoxP3+ T regulatory cells. Int. Immunopharmacol. *7*, 1819–1824. https://doi.org/10.1016/j.intimp.2007.08.027.
53. Morou, A., Brunet-Ratnasingham, E., Dubé, M., Charlebois, R., Mercier, E., Darko, S., Brassard, N., Nganou-Makamdop, K., Arumugam, S., Gendron-Lepage, G., et al. (2019). Altered differentiation is central to HIV-specific CD4(+) T cell dysfunction in progressive disease. Nat. Immunol. *20*, 1059–1070. https://doi.org/10.1038/s41590-019-0418-x.
54. Limagne, E., Thibaudin, M., Euvrard, R., Berger, H., Chalons, P., Végan, F., Humblin, E., Boidot, R., Rébé, C., Derangère, V., et al. (2017). Sirtuin-1 Activation Controls Tumor Growth by Impeding Th17 Differentiation via STAT3 Deacetylation. Cell Rep. *19*, 746–759. https://doi.org/10.1016/j.celrep.2017.04.004.
55. Caetano, D.G., de Paula, H.H.S., Bello, G., Hoagland, B., Villela, L.M., Grinsztejn, B., Veloso, V.G., Morgado, M.G., Guimarães, M.L., and Côrtes, F.H. (2020). HIV-1 elite controllers present a high frequency of activated regulatory T and Th17 cells. PLoS One *15*, e0228745. https://doi.org/10.1371/journal.pone.0228745.
56. Wacleche, V.S., Goulet, J.P., Gosselin, A., Monteiro, P., Soudeyns, H., Fromentin, R., Jenabian, M.A., Vartanian, S., Deeks, S.G., Chomont, N., et al. (2016). New insights into the heterogeneity of Th17 subsets contributing to HIV-1 persistence during antiretroviral therapy. Retrovirology *13*, 59. https://doi.org/10.1186/s12977-016-0293-6.
57. Wiche Salinas, T.R., Zhang, Y., Sarnello, D., Zhyvoloup, A., Marchand, L.R., Fert, A., Planas, D., Lodha, M., Chatterjee, D., Karwacz, K., et al. (2021). Th17 cell master transcription factor RORC2 regulates HIV-1 gene expression and viral outgrowth. Proc. Natl. Acad. Sci. USA *118*, e2105927118. https://doi.org/10.1073/pnas.2105927118.
58. Olety, B., Peters, P., Wu, Y., Usami, Y., and Göttlinger, H. (2021). HIV-1 propagation is highly dependent on basal levels of the restriction factor BST2. Sci. Adv. *7*, eabj7398. https://doi.org/10.1126/sciadv.abj7398.
59. Weichhart, T., Hengstschläger, M., and Linke, M. (2015). Regulation of innate immune cell function by mTOR. Nat. Rev. Immunol. *15*, 599–614. https://doi.org/10.1038/nri3901.
60. Chamontin, C., Bossis, G., Nisole, S., Arhel, N.J., and Maarifi, G. (2021). Regulation of Viral Restriction by Post-Translational Modifications. Viruses *13*, 2197. https://doi.org/10.3390/v13112197.
61. Li, S.X., Barrett, B.S., Guo, K., and Santiago, M.L. (2016). Tetherin/BST-2: Restriction Factor or Immunomodulator? Curr. HIV Res. *14*, 235–246. https://doi.org/10.2174/1570162x14999160224102752.
62. Singh, R., Ramsuran, V., Naranbhai, V., Yende-Zuma, N., Garrett, N., Mlisana, K., Dong, K.L., Walker, B.D., Abdool Karim, S.S., Carrington, M., and Ndung'u, T. (2021). Epigenetic Regulation of BST-2 Expression Levels and the Effect on HIV-1 Pathogenesis. Front. Immunol. *12*, 669241. https://doi.org/10.3389/fimmu.2021.669241.
63. Weinelt, J., and Neil, S.J.D. (2014). Differential sensitivities of tetherin isoforms to counteraction by primate lentiviruses. J. Virol. *88*, 5845–5858. https://doi.org/10.1128/JVI.03818-13.
64. Venkatesh, S., and Bieniasz, P.D. (2013). Mechanism of HIV-1 virion entrapment by tetherin. PLoS Pathog. *9*, e1003483. https://doi.org/10.1371/journal.ppat.1003483.
65. Kueck, T., Foster, T.L., Weinelt, J., Sumner, J.C., Pickering, S., and Neil, S.J.D. (2015). Serine Phosphorylation of HIV-1 Vpu and Its Binding to Tetherin Regulates Interaction with Clathrin Adaptors. PLoS Pathog. *11*, e1005141. https://doi.org/10.1371/journal.ppat.1005141.
66. Jones, P.H., and Okeoma, C.M. (2013). Phosphatidylinositol 3-kinase is involved in Toll-like receptor 4-mediated BST-2/tetherin regulation. Cell. Signal. *25*, 2752–2761. https://doi.org/10.1016/j.cellsig.2013.08.042.
67. Hatok, J., and Racay, P. (2016). Bcl-2 family proteins: master regulators of cell survival. Biomol. Concepts *7*, 259–270. https://doi.org/10.1515/bmc-2016-0015.
68. Ren, Y., Huang, S.H., Patel, S., Alberto, W.D.C., Magat, D., Ahimovic, D., Macedo, A.B., Durga, R., Chan, D., Zale, E., et al. (2020). BCL-2 antagonism sensitizes cytotoxic T cell-resistant HIV reservoirs to elimination ex vivo. J. Clin. Invest. *130*, 2542–2559. https://doi.org/10.1172/JCI132374.
69. Chandrasekar, A.P., Cummins, N.W., Natesampillai, S., Misra, A., Alto, A., Laird, G., and Badley, A.D. (2022). The BCL-2 Inhibitor Venetoclax Augments Immune Effector Function Mediated by Fas Ligand, TRAIL, and Perforin/Granzyme B, Resulting in Reduced Plasma Viremia and Decreased HIV Reservoir Size during Acute HIV Infection in a Humanized Mouse Model. J. Virol. *96*, e0173022. https://doi.org/10.1128/jvi.01730-22.
70. Arandjelovic, P., Kim, Y., Cooney, J.P., Preston, S.P., Doerflinger, M., McMahon, J.H., Garner, S.E., Zerbato, J.M., Roche, M., Tumpach, C., et al. (2023). Venetoclax, alone and in combination with the BH3 mimetic S63845, depletes HIV-1 latently infected cells and delays rebound in humanized mice. Cell Rep. Med. *4*, 101178. https://doi.org/10.1016/j.xcrm.2023.101178.
71. Chandrasekar, A.P., and Badley, A.D. (2022). Prime, shock and kill: BCL-2 inhibition for HIV cure. Front. Immunol. *13*, 1033609. https://doi.org/10.3389/fimmu.2022.1033609.
72. Kim, Y., Anderson, J.L., and Lewin, S.R. (2018). Getting the "Kill" into "Shock and Kill": Strategies to Eliminate Latent HIV. Cell Host Microbe *23*, 14–26. https://doi.org/10.1016/j.chom.2017.12.004.
73. Landovitz, R.J., Scott, H., and Deeks, S.G. (2023). Prevention, treatment and cure of HIV infection. Nat. Rev. Microbiol. *21*, 657–670. https://doi.org/10.1038/s41579-023-00914-1.
74. Galão, R.P., Le Tortorec, A., Pickering, S., Kueck, T., and Neil, S.J. (2012). Innate sensing of HIV-1 assembly by Tetherin induces NFkappaB-dependent proinflammatory responses. Cell Host Microbe *12*, 633–644. https://doi.org/10.1016/j.chom.2012.10.007.
75. Pham, T.N.Q., Lukhele, S., Hajjar, F., Routy, J.P., and Cohen, É.A. (2014). HIV Nef and Vpu protect HIV-infected CD4+ T cells from antibody-mediated cell lysis through down-modulation of CD4 and BST2. Retrovirology *11*, 15. https://doi.org/10.1186/1742-4690-11-15.
76. Pham, T.N.Q., Lukhele, S., Dallaire, F., Perron, G., and Cohen, É.A. (2016). Enhancing Virion Tethering by BST2 Sensitizes Productively and Latently HIV-infected T cells to ADCC Mediated by Broadly Neutralizing Antibodies. Sci. Rep. *6*, 37225. https://doi.org/10.1038/srep37225.
77. Richard, J., Prevost, J., von Bredow, B., Ding, S., Brassard, N., Medjahed, H., Coutu, M., Melillo, B., Bibollet-Ruche, F., Hahn, B.H., et al. (2017). BST-2 Expression Modulates Small CD4-Mimetic Sensitization of HIV-1-Infected Cells to Antibody-Dependent Cellular Cytotoxicity. J. Virol. *91*, 10–1128. https://doi.org/10.1128/JVI.00219-17.
78. Arias, J.F., Heyer, L.N., von Bredow, B., Weisgrau, K.L., Moldt, B., Burton, D.R., Rakasz, E.G., and Evans, D.T. (2014). Tetherin antagonism by Vpu protects HIV-infected cells from antibody-dependent cell-mediated cytotoxicity. Proc. Natl. Acad. Sci. USA *111*, 6425–6430. https://doi.org/10.1073/pnas.1321507111.
79. Alvarez, R.A., Hamlin, R.E., Monroe, A., Moldt, B., Hotta, M.T., Rodriguez Caprio, G., Fierer, D.S., Simon, V., and Chen, B.K. (2014). HIV-1 Vpu antagonism of tetherin inhibits antibody-dependent cellular cytotoxic responses by natural killer cells. J. Virol. *88*, 6031–6046. https://doi.org/10.1128/JVI.00449-14.
80. Prévost, J., Pickering, S., Mumby, M.J., Medjahed, H., Gendron-Lepage, G., Delgado, G.G., Dirk, B.S., Dikeakos, J.D., Sturzel, C.M., Sauter, D., et al. (2019). Upregulation of BST-2 by Type I Interferons Reduces the Capacity of Vpu To Protect HIV-1-Infected Cells from NK Cell Responses. mBio *10*, 10–1128. https://doi.org/10.1128/mBio.01113-19.
81. Moldt, B., Le, K.M., Carnathan, D.G., Whitney, J.B., Schultz, N., Lewis, M.G., Borducchi, E.N., Smith, K.M., Mackel, J.J., Sweat, S.L., et al. (2016). Neutralizing antibody affords comparable protection against vaginal and rectal simian/human immunodeficiency virus challenge in macaques. AIDS *30*, 1543–1551. https://doi.org/10.1097/QAD.0000000000001102.
82. Collins, D.R., Gaiha, G.D., and Walker, B.D. (2020). CD8(+) T cells in HIV control, cure and prevention. Nat. Rev. Immunol. *20*, 471–482. https://doi.org/10.1038/s41577-020-0274-9.
83. McBrien, J.B., Kumar, N.A., and Silvestri, G. (2018). Mechanisms of CD8(+) T cell-mediated suppression of HIV/SIV replication. Eur. J. Immunol. *48*, 898–914. https://doi.org/10.1002/eji.201747172.
84. Araki, K., Turner, A.P., Shaffer, V.O., Gangappa, S., Keller, S.A., Bachmann, M.F., Larsen, C.P., and Ahmed, R. (2009). mTOR regulates memory CD8 T-cell differentiation. Nature *460*, 108–112. https://doi.org/10.1038/nature08155.
85. Cha, J.H., Yang, W.H., Xia, W., Wei, Y., Chan, L.C., Lim, S.O., Li, C.W., Kim, T., Chang, S.S., Lee, H.H., et al. (2018). Metformin Promotes Antitumor Immunity via Endoplasmic-Reticulum-Associated

Degradation of PD-L1. Mol. Cell *71*, 606–620.e7. https://doi.org/10.1016/j.molcel.2018.07.030.

86. Chew, G.M., Padua, A.J.P., Chow, D.C., Souza, S.A., Clements, D.M., Corley, M.J., Pang, A.P.S., Alejandria, M.M., Gerschenson, M., Shikuma, C.M., and Ndhlovu, L.C. (2021). Effects of Brief Adjunctive Metformin Therapy in Virologically Suppressed HIV-Infected Adults on Polyfunctional HIV-Specific CD8 T Cell Responses to PD-L1 Blockade. AIDS Res. Hum. Retroviruses *37*, 24–33. https://doi.org/10.1089/AID.2020.0172.
87. Chatterjee, D., Zhang, Y., Ngassaki-Yoka, C.D., Dutilleul, A., Khalfi, S., Hernalsteens, O., Wiche Salinas, T.R., Dias, J., Chen, H., Smail, Y., et al. (2023). Identification of aryl hydrocarbon receptor as a barrier to HIV-1 infection and outgrowth in CD4(+) T cells. Cell Rep. *42*, 112634. https://doi.org/10.1016/j.celrep.2023.112634.
88. Palella, F.J., Hart, R., Armon, C., Tedaldi, E., Yangco, B., Novak, R., Battalora, L., Ward, D., Li, J., and Buchacz, K.; HIV Outpatient Study HOPS (2019). Non-AIDS comorbidity burden differs by sex, race, and insurance type in aging adults in HIV care. AIDS *33*, 2327–2335. https://doi.org/10.1097/QAD.0000000000002349.
89. Bounou, S., Leclerc, J.E., and Tremblay, M.J. (2002). Presence of host ICAM-1 in laboratory and clinical strains of human immunodeficiency virus type 1 increases virus infectivity and CD4(+)-T-cell depletion in human lymphoid tissue, a major site of replication in vivo. J. Virol. *76*, 1004–1014. https://doi.org/10.1128/jvi.76.3.1004-1014.2002.
90. Boulassel, M.R., Spurll, G., Rouleau, D., Tremblay, C., Edwardes, M., Sekaly, R.P., Lalonde, R., and Routy, J.P. (2003). Changes in immunological and virological parameters in HIV-1 infected subjects following leukapheresis. J. Clin. Apher. *18*, 55–60. https://doi.org/10.1002/jca.10051.
91. Fromentin, R., DaFonseca, S., Costiniuk, C.T., El-Far, M., Procopio, F.A., Hecht, F.M., Hoh, R., Deeks, S.G., Hazuda, D.J., Lewin, S.R., et al. (2019). PD-1 blockade potentiates HIV latency reversal ex vivo in CD4(+) T cells from ART-suppressed individuals. Nat. Commun. *10*, 814. https://doi.org/10.1038/s41467-019-08798-7.

STAR★METHODS

KEY RESOURCES TABLE

REAGENT or RESOURCE	SOURCE	IDENTIFIER
Antibodies		
Purified no azide (NA)/low endotoxin (LE) Mouse Anti-Human CD3 (Clone UCHT1)	BD	Cat#555329; RRID: AB_395736
Purified NA/LE Mouse Anti-Human CD28 (Clone CD28.2)	BD	Cat#555725; RRID: AB_396068
Mouse anti-human CD3 Pacific Blue (Clone UCHT1)	BD	Cat#558117; RRID: AB_397038
Mouse anti-human CD4 Alexa Fluor (Clone RPA-T4)	BD	Cat#561030; RRID: AB_10563215
Mouse anti-human CD8 FITC (Clone 130-080-601)	Miltenyi	Cat#130-080-601; RRID: AB_244336
Mouse anti-human CCR6 PE (Clone 11A9)	BD	Cat#559562; RRID: AB_397273
Mouse anti-human CD45RA allophytocyanin hilite (APC-H7) (Clone HI100)	BD	Cat#560674; RRID: AB_1727497
Mouse anti-human CXCR4 APC (Clone 12G5)	eBiosciences	Cat#17-9999-42; RRID: AB_1724113
Mouse anti-human CD317 (BST-2) BV421 (Clone Y129)	BD	Cat#566381; RRID: AB_2744363
Hamster anti-human Bcl-2 FITC	BD	Cat#554234; RRID: AB_395319
HIV-1 core (p24) antigen-FITC (Clone KC57)	Beckman Coulter	Cat#6604665
HIV-1 core (p24) antigen-RD1 (Clone KC57)	Beckman Coulter	Cat#6604667; RRID: AB_1575989
Mouse anti-human RORC2 Alex Fluor 647 (Clone Q21-559)	BD	Cat#563620; RRID: AB_2738324
Mouse anti-human IL-17A PE (Clone eBio64DEC17)	eBiosciences	Cat#12-7179-42; RRID: AB_1724136
Goat anti-Human IgG Secondary Antibody, Alexa Fluor 647	Invitrogen	Cat#A-21445; RRID: AB_2535862
Anti-phospho-Ribosomal Protein S6 (Ser240/Ser244)	EMD Millipore	Cat#07 2113
Phospho-mTOR (Ser2448)	Cell Signaling	Cat#2971; RRID: AB_330970
Secondary antibody anti-Rabbit IgG HRP-linked	Cell Signaling	Cat#7074; RRID: AB_2099233
Monoclonal Mouse Anti-β-Actin antibody	Millipore Sigma	Cat#A5441; RRID: AB_476744
Goat anti-Mouse IgG (H + L) Secondary Antibody, HRP	Invitrogen	Cat#32430; RRID: AB_1185566
Bacterial and virus strains		
One Shot Stbl3 Chemically Competent E. coli	Life Technologies	C737303
NL4.3BaL HIV plasmid	From Dr. Michel tremblay, Université Laval, Québec, Canada	N/A
pHEF Expressing Vesicular Stomatitis Virus (VSV-G) plasmid	NIH HIV Reagent Program, Division AIDS, NIAID (Contribution of Dr. Lung Ji Chang)	Cat#ARP-4693
HIV-1 NL4-3 ΔEnv EGFP Reporter Vector	NIH HIV Reagent Program, Division of AIDS, NIAID (Contribution Dr. Haili Zhang, Dr. Yan Zhou and Dr. Robert Siliciano)	Cat#ARP11100
Biological samples		
Leukaphereses of ART treated people living with HIV and HIV-uninfected people	Recruited at the Montreal Chest Institute, McGill University Health Center and Center Hospitalier de l'Université de Montréal with the help of Dr Jean-Pierre Routy's group	N/A
Chemicals, peptides, and recombinant proteins		
rhIL-2	R&D Systems	Cat#202-IL-050
1,1-Dimethylbiguanide, Hydrochloride (Metformin)	Santa Cruz	Cat#sc-202000

(*Continued on next page*)

Continued

REAGENT or RESOURCE	SOURCE	IDENTIFIER
Sapanisertib (INK128)	Cayman Chemical	Cat#11811-1
Saquinavir	NIH HIV Reagent Program, Division of AIDS, NIAID (Contribution DAIDS/NIAID)	Cat#ARP-4658
Raltegravir	NIH HIV Reagent Program, Division of AIDS, NIAID (Contribution DAIDS/NIAID)	Cat#ARP-11680
Radioimmunoprecipitation Assay Buffer (RIPA) 10X	Cell Signaling	Cat#9806S
Phosphatase Inhibitor (PhosSTOP)	Milipore Sigma	Cat#4906845001
Complete, Mini, EDTA-free protease inhibitor	Milipore Sigma	Cat#11836170001
Clarity and Clarity Max ECL Western Blotting Substrates	Bio-Rad	Cat#1705062S
ReBlot Plus Strong Antibody Stripping Solution	Sigma	Cat#2504
Sodium Bicarbonate ($NaHCO_3$)	Sigma	Cat#S5761
Sodium Carbonate (Na_2CO_3)	Sigma	Cat#223530-500G
Thimerosal	Sigma	Cat#T5125-10G
Phosphate Buffered Saline (PBS)	Thermo Fisher	Cat#10010023
Tween 20	Fisher Scientific	Cat#BP337-500
Triton X-100	Sigma	Cat#X100-500mL
Trypan Blue	Thermo Fisher	Cat#15250061
Bovine Serum Albumin (BSA)	BioShop	Cat#ALB001.500
Streptavidin Horseradish Peroxidase (Strep-HRP)	Fisher Scientific	Cat#65R-S104PHRP
3,3′,5,5′-Tetramethylbenzidine (TMB)	Quimigen	Cat#42R-TB10265R-S104PHRP
Phosphoric Acid (H_3PO_4)	Sigma	Cat#PX0996
Nonidet P-40	Bioshop	Cat#NON505
Tris HCl	BioShop	Cat#TRS002.500
Proteinase K	Fisher Scientific	Cat#25530-015
Molecular Grade Water (H_2O)	Wisent	Cat#809-115-CL
Guanidine-HC;	Promega	H5381
Trypsin EDTA with phenol red	Wisent	Cat#075-350
Methanol 99,98%	Fisher Scientific	Cat#BPA4084
4X Laemmli Sample Buffer	Bio-Rad	Cat#1610747
2-Mercaptoethanol	Sigma	Cat#M6250
Precision Plus Protein Dual Color Standards	Bio-Rad	Cat#1610374
Glycine	BioShop	Cat#GLN001.500
Sodium Chloride	BioShop	Cat#SOD002
30% Bis-acrylamide Solution	Bioshop	Cat#ACR010.500
UltraPure Tris Buffer	Thermo Fisher	Cat#15504-020
Sodium Dodecyl Sulfate (SDS)	Bio-Rad	Cat#1610302
N,N,N′,N′-Tetramethyl Ethylenediamine (TEMED)	Sigma	Cat#8087420005
Ammonium Persulfate (APS)	Bioshop	Cat#AMP001.100
Formaldehyde solution 37 wt. % in H_2O	Sigma	Cat#F1635-500ML
Sodium Azide	Bioshop	Cat#SAZ001.250
Fetal Bovine Serum (FBS)	Wisent	Cat#091-150
Dimethyl Sulfoxide (DMSO)	Sigma	Cat#34869-500mL
RPMI 1640 Medium (RPMI)	Thermo Fisher	Cat#11875119
Penicillin/streptomycin (PenStep)	Thermo Fisher	Cat#15140122

(*Continued on next page*)

Continued

REAGENT or RESOURCE	SOURCE	IDENTIFIER
Lymphocyte Separation Medium (LSM)	Wisent	Cat#305-010-CL
EDTA	Bioshop	Cat#EDT001.1
Opti-MEM	Gibco	Cat#31985070
Critical commercial assays		
p24 Enzyme-linked Immunosorbent Assay (ELISA)	Homemade. Hybridome provided by Dr. Michel J. Tremblay (Bounou et al.[89])	N/A
QuantiTect SYBR Green RT-PCR Kit	Qiagen	Cat#204243
10X PCR Buffer/Magnesium Chloride ($MgCl_2$) Buffer/ Thermus Aquaticus (TAQ) Polymerase	Thermo Fisher	Cat#18038067
LC480 probe master mix	Roche	Cat#4707494001
QuantiTect SYBR Green RT-PCR Kit	Qiagen	Cat#204243
Deoxynucleoside Triphosphates (dNTP)	Thermo Fisher	Cat#10297018
Wizard Plus DNA Purification System	Fisher Scientific	PR-A7100
EndoFree Plasmid Maxi Kit	Qiagen	12362
EasySep Memory $CD4^+$ T cell Isolation Kit, human	StemCell Technology	Cat#19157
Rneasy Plus Mini Kit	Qiagen	Cat#74136
Detergent Compatible (DC) Protein Assay	Bio-Rad	Cat#5000111
Foxp3 transcription factor staining buffer set	eBioscience	Cat # 00-5523-00
X-tremeGENE 9 kit	Roche	Cat#06 365 779 001
LIVE/DEAD Fixable Aqua Dead Cell Stain Kit (405 nm excitation)	Thermo Fisher	Cat#L34957
Experimental models: cell lines		
293T	ATCC	Cat#CRL-3216
ACH-2	NIH HIV Reagent Program	Cat#ARP-349
Oligonucleotides		
See Table S2: Oligonucleotides	See Table S2: Oligonucleotides	See Table S2: Oligonucleotides
Software and algorithms		
FlowJo version 10	BD	https://www.flowjo.com/
GraphPad Prism 9.0.1	GraphPad	https://www.graphpad.com/
Image Lab	Bio-Rad	https://www.bio-rad.com/en-ca/product/image-lab-software?ID=KRE6P5E8Z
Other		
Immobilon-PSQ Polyvinylidene Difluoride (PVDF)	Sigma	Cat#ISEQ00010
Resource availability: data availability		
Uncropped western blot (Figures S1A and S1C)	Mendeley Data	Fert, Augustine (2024), "Metformin Facilitates Viral Reservoir Reactivation and their Recognition by Anti-HIV-1 Envelope Antibodies. Fert et al.", Mendeley Data, V1, https://doi.org/10.17632/trckskyvcw.1

RESOURCE AVAILABILITY

Lead contact

Further information and requests for resources and reagents should be directed to and will be fulfilled by the lead contact, Petronela Ancuta (petronela.ancuta@umontreal.ca).

Materials availability

This study did not generate new unique reagents.

Data and code availability

- Uncropped western blot membrane displayed in Figures S1A and S1C have been deposited at the database Mendeley Data (https://data.mendeley.com) and are publicly available as of the date of publication. Accession number is listed in the key resources table.
- This study did not generate new codes
- Any additional information required to reanalyze the data reported in this paper is available from the lead contact upon request.

Ethics statement

Study participants were recruited at the Montreal Chest Institute, McGill University Health Center, and Center Hospitalier de l'Université de Montréal (Montreal, Québec, Canada), in compliance with the principles included in the Declaration of Helsinki. This study received approval from the Institutional Review Board (IRB) of the McGill University Health Center and the CHUM Research Center, Montreal, Quebec, Canada. All participants signed a written informed consent and agreed with the publication of the results.

Study participants

This study was performed using Peripheral Blood Mononuclear Cells (PBMCs) from ART-treated PWH (n = 13) and HIV-uninfected (n = 15) study participants. PBMCs were isolated by gradient density centrifugation from leukapheresis and maintained frozen in liquid nitrogen until use.[90] Clinical parameters of study participants are included in Table 1 for PWH and Table S1 for HIV-uninfected donors.

Memory CD4$^+$ T cell sorting

Memory CD4$^+$ T-cells were isolated from PBMCs of HIV-uninfected and ART-treated PWH by negative selection using the EasySep Human Memory CD4$^+$ T cell Enrichment Kit (StemCell Technology), following the manufacturer recommendation. The cell purity after sorting was >95%, as determined upon staining with CD3, CD4, CD45RA and CD8 Abs and flow cytometry analysis (BD LSRII).

Flow cytometry analysis

For surface staining, cells were incubated for 30 min at 4°C in PBS 1X buffer containing 10% FBS (Wisent), 0.02% NaN3 and fluorescence-conjugated antibodies against CD3, CD4, CD8, CCR6, CD45RA, CXCR4 and BST2 (Table S1), using a protocol we previously reported.[20,57] Live/Dead Fixable Aqua Dead cells stain Kit was used to exclude dead cells (Invitrogen). Intracellular/nuclear staining was performed using the FoxP3 transcription factor staining buffer kit (eBioscience) and fluorescence-conjugated antibodies against HIV-p24 KC57, RORC2 and Bcl-2 (key resources table). Flow cytometry acquisition of stained cells was performed on a BD LSRII cytometer. Flow cytometry analysis was performed using the BD Diva and FlowJo version 10. The positivity gate for RORC2 were placed using the fluorescence minus one (FMO) strategy. The positivity gate for HIV-p24 (KC57) were placed using uninfected memory CD4$^+$ T-cells.

Cell culture and activation

For TCR triggering of primary memory CD4$^+$ T-cells, cells were cultured in RPMI1640 (GIBCO) cell-culture media (10% FBS, 1% Penicillin/Streptomycin (GIBCO) at 1 × 10^6 cells/mL in the presence of immobilized CD3 antibodies (1 μg/mL; BD Biosciences) and soluble CD28 antibodies (1 μg/mL; BD Biosciences).

Compounds

The following drugs were used to treat primary CD4$^+$ T-cells: metformin (0.1; 0.5; 1 and 5 mM) (1,1-Dimethylbiguanide, HydrochlorideSanta Cruz); INK128 (50 μM) (Cayman); Saquinavir (5 μM) (NIH HIV Reagent Program), and Raltegravir (0.2 μM) (NIH HIV Reagent Program).

HIV viral stocks

In this study, the following HIV-1 viruses were used *(i)* replication-competent CCR5 using (R5) NL4.3BAL and *(ii)* single-round VSVG-HIV-GFP, an *env*-deficient NL4.3 provirus pseudotyped with the VSV-G envelope and encoding for *gfp* in place of *env*. The NL4.3BaL HIV plasmid was provided by Michel Tremblay, Université Laval, Quebec, Canada, originating from Roger J. Pomerantz, Thomas Jefferson University, Philadelphia, PA. The plasmid pHEF Expressing Vesicular Stomatitis Virus (VSV-G) (ARP-4693) was obtained through the NIH HIV Reagent Program, Division of AIDS, NIAID, NIH, contributed by Dr. Lung-Ji Chang. The HIV vector containing the NL4-3 backbone encoding for enhanced green fluorescent protein (EGFP) in place of the Envelope (Env) (NL4.3EGFPΔEnv), and encoding for functional Nef and Vpu, was obtained through the NIH HIV Reagent Program, Division of AIDS, NIAID, NIH, contributed by Dr. Haili Zhang, Dr. Yan Zhou and Dr. Robert Siliciano. The plasmids were amplified upon bacterial transformation by MiniPrep (Promega) and MaxiPrep (Qiagen) following the manufacturer recommendation. The plasmid NL4.3Bal HIV-1 was transfected in 293T cells (*ATCC*) in order to produce the CCR5-tropic replication-competent NL4.3Bal HIV-1 viral stock. *The 293T cell stocks were tested for Mycoplasma (ThermoFisher Scientific).* The plasmids VSV-G and NL4-3 ΔEnv EGFP were transfected together in a ratio 1:3 in 293T-cells. To perform the transfection in 293T-cells, using the X-tremeGENE 9 kit

(Roche), according to manufacturer's recommendation. Cell-culture supernatant containing the virus was collected 72 h post-transfection. The NL4.3Bal HIV stock obtained on 293T-cells was passed once on TCR-activated memory $CD4^+$ T-cells and the cell-culture supernatant was collected at day 12 post-infection. The HIV viral stocks were quantified by HIV-p24 ELISA and the quantity needed for optimal infection was determined by titration on TCR-activated memory $CD4^+$ T-cells.

HIV-1 infection *in vitro*

HIV-1 infection *in vitro* was performed as we previously reported.[57] Memory $CD4^+$ T-cells were stimulated by CD3/CD28 Abs for 3 days prior infection. Cells were exposed to NL4.3BAL (50 ng HIV-p24/10^6 cells) for 3 h at 37°C and homogenized every 30 min, or VSVG-HIV-GFP (100 ng HIV-p24/10^6 cells) and spinoculated for 1 h at 300 g at room temperature. Unbound virions were removed by extensive washing with RPMI1640 10%FBS, 1%PS. Cells were cultured in the presence of IL-2 (5 ng/mL; R&D Systems) at 37°C for 12 and 3 days for NL4.3BAL and VSVG-HIV-GFP, respectively. A fraction of cells collected at day 3 post-infection was used for nested real-time PCR quantification of HIV-DNA. Cell-culture supernatants were harvested and productive infection was measured by HIV-p24 ELISA, using homemade Abs,[89,91] and flow cytometry analysis upon surface CD4 and intracellular HIV-p24 staining. Productively infected T-cells were identified based on their $CD4^{low}$HIV-$p24^+$ phenotype, with CD4 downregulation being indicative of productive infection.[33,34]

Viral Outgrowth Assay (VOA)

To measure replication-competent VRs, a simplified viral outgrowth assay was performed using a protocol developed in our lab.[38] Succinctly, memory $CD4^+$ T-cells from ART-treated PWH were cultured at 1x10^6cells/well in RPMI1640, 10%FBS, 1% PS cell-culture media in 48-well plates in the presence of immobilized CD3 Abs and soluble CD28 Abs (1 μg/mL). At day 3, cells were washed to remove the CD3/CD28 Abs. Cells from each well were split into two new wells for optimal cell density (typically 1-2 × 10^6 cells/mL/well) and cultured in the presence of IL-2 (5 ng/mL). The splitting procedure was repeated with media being refreshed every 3 days. The VOA was performed in the presence or the absence of metformin (1 mM), INK128 (50 μM) and antiretroviral drugs (ARVs; Saquinavir at 5 μM and Raltegravir at 0.2 μM). At day 12, one original replicate generated 8 splitting replicates, from which cells were harvested for the quantification of intracellular HIV-p24 expression by flow cytometry, as well as HIV-DNA by PCR. Cell-culture supernatants were collected every 3 days for HIV-p24 level quantification by ELISA.

Quantification of early, late reverse transcript and integrated HIV-DNA

Early and late HIV-1 reverse transcripts, as well as integrated HIV-DNA levels were quantified using specific primers and probes (Table S2), as we previously described.[20,87] Briefly, cell lysates, generated by proteinase K digestion, were used to quantify HIV-DNA copies. Early reverse transcripts were amplified using primers specific for the RU5 region of the HIV genome, using SYBR green real-time nested PCR (Qiagen). Gag and integrated HIV-DNA, as well as CD3 DNA (used to normalize HIV-DNA expression per number of cells) were amplified using specific primers (Table S2) and nested real-time PCR. The first PCR round performed with both HIV and CD3 primers was followed by a second round of PCR performed with specific internal primers and probes on the LightCycler 480II (Roche) (Table S2). Results are expressed as HIV-DNA copies per million cells, upon normalization to CD3 copies. For all PCR quantifications, ACH2 cells (NIH HIV Reagent Program) carrying one copy of integrated HIV-DNA per cells, were used as a standard curve.

Anti-HIV-1 envelope antibodies recognition of productively HIV-infected T-cells

Memory $CD4^+$ T-cells harvested at Day 12 of VOA were analyzed by flow cytometry for the binding of a panel human Abs directed against the HIV-1 Env. The following antibodies were used: anti-gp41 F240; anti-cluster A A32, anti-coreceptor binding site 17b; anti-CD4 binding site VRC03, 3BNC117; anti-gp120 outer domain 2G12; the gp120-gp41 interface PGT151 and anti-V3 glycan PGT121, PGT126, 101074. The goat anti-human IgGs conjugated with Alexa Fluor 647 (Invitrogen) were used as a secondary Abs to determine the levels of anti-HIV-gp120 Abs binding. Then the cells were stained on the surface with CD4-Alexa Fluor 700 Abs and intracellularly with HIV-p24-FITC Abs (key resources table). Productively infected T-cells were identified based on their $CD4^{low}$HIV-$p24^+$ phenotype. The viability dye was used to exclude dead cells from the analysis.

HIV-1 env antibody production

FreeStyle 293F cells (Thermo Fisher Scientific) were grown in FreeStyle 293F medium (Thermo Fisher Scientific) to a density of 1 × 10^6 cells/mL at 37°C with 8% CO_2 with regular agitation (150 rpm). Cells were transfected with plasmids expressing the light and heavy chains of A32 (kindly provided by James Robinson); VRC03 (kindly provided by John Mascola); 3BNC117, 10–1074 (kindly provided by Michel Nussenzweig); F240, 2G12, 17b (NIH AIDS Reagent Program); PGT121, PGT126, PGT151 (IAVI), using ExpiFectamine 293 transfection reagent, as directed by the manufacturer (Thermo Fisher Scientific). One week later, the cells were pelleted and discarded. The supernatants were filtered (0.22-μm-pore-size filter), and antibodies were purified by protein A affinity columns, as directed by the manufacturer (Cytiva, Marlborough, MA, USA).

Western blot

The visualization of total and phosphorylated mTOR and S6 ribosomal proteins was performed using protocols established in the laboratory.[20] Cells were lysed with RIPA buffer (Cell Signaling) containing phosphatase inhibitors and protease inhibitors (Milipore Sigma) for 5 min at 4°C and sonicated 3 times for 5 s on ice. Lysed pellets were centrifuged at 14,000 g for 10 min to remove cell debris. Proteins

were quantified using the kit DM Protein Assay (Bio-Rad). Loading of proteins (10 μg/well) was performed onto a 7% acrylamide SDS gel for mTOR and 15% for S6 ribosomal and electrophoretic migration was performed (1h10 at 150V). Migrated proteins were transferred by electrophoresis on activated PVDF membrane (1 h at 100V). Membranes were blocked for 45 min at room temperature with TBST 5% BSA, 0.1% Tween buffer. To measure phosphorylated proteins, membranes were bloated with primary Abs against Phosphorylated Ribosomal S6 (EMD Milipore) and Phosphorylated mTOR (Cell Signaling) Abs overnight at 4°C. Then membranes were washed with TBST 0.1 %Tween buffer and incubated with secondary antibody anti-Rabbit IgG HRP-linked (Cell Signaling) for 1 h at room temperature. Proteins were revealed with Clarity Max Western ECL Substrate, (Bio-Rad). For total mTOR and S6, the same membranes were stripped with Re-Blot Plus Strong Solution (EMD Milipore) and re-bloated with the appropriate primary and secondary Abs. For β-actin, the same membranes were stripped with Re-Blot Plus Strong Solution (EMD Milipore) and re-bloated with the primary anti-β-actin Abs (Sigma Aldrich) and HRP conjugated-secondary Abs (Invitrogen).

STATISTICAL ANALYSIS

Statistical analyses were performed with GraphPad Prism 9.0.1. Statistical tests used are indicated in the figure legends and *p*-values are indicated on the graphs. *P*-values ≤ 0.05 were considered statistically significant. When the general statistical tests (i.e., Friedman) reached the statistical threshold (*p*-values ≤ 0.05), the uncorrected Dunn's multiple comparison test was performed, with *p*-values indicated within the graphs to indicate statistical significance between conditions.